

# Bipartite and tripartite entanglement in pure dephasing relativistic spin-boson model

Kensuke Gallock-Yoshimura<sup>1,2,\*</sup> and Erickson Tjoa<sup>3,†</sup>

<sup>1</sup>*Department of Information and Communication Engineering,  
Graduate School of Information Science and Technology,*

*The University of Tokyo, 7-3-1 Hongo, Bunkyo-ku, Tokyo 113-8656, Japan*

<sup>2</sup>*Department of Physics, Kyushu University, 744 Motoooka, Nishi-Ku, Fukuoka 819-0395, Japan*

<sup>3</sup>*Max-Planck-Institut für Quantenoptik, Hans-Kopfermann-Straße 1, D-85748 Garching, Germany*

(Dated: July 21, 2025)

We study non-perturbatively the entanglement generation between two and three emitters in an exactly solvable relativistic variant of the spin-boson model, equivalent to the time-independent formulation of the Unruh-DeWitt detector model. We show that (i) (highly) entangled states of the two emitters require interactions very deep into the light cone, (ii) the mass of the field can generically improve the entanglement generation, (iii) unlike the bipartite case where it is possible to generate close to maximally entangled states via the spin-boson interactions, the generation of genuine tripartite entanglement is non-perturbatively hard even at sufficiently long times. Result (iii), in particular, suggests that probing the multipartite entanglement of a relativistic quantum field non-perturbatively requires either different probe-based techniques or variants of the UDW model. Along the way we provide the regularity conditions for the  $N$ -emitter model to have well-defined ground states in the Fock space.

## I. INTRODUCTION

The Unruh-DeWitt (UDW) model [1, 2] is a well-known model of light-matter interaction that has been used to study relativistic phenomena predicted from quantum field theory (QFT) in curved spacetimes, such as the Unruh and Hawking effects [1–7]. The model has been generalized in different ways and applied to many different contexts to study entanglement and communication (see, e.g., [8–28]). In [29], it was argued that it is sometimes useful to view the UDW model as a relativistic variant of the spin-boson (SB) model [30–32]. Physically, the main difference between the standard UDW model and the relativistic spin-boson (RSB) model is that the latter is described by a time-independent Hamiltonian — as a closed system — while the former is time-dependent. Terminology-wise, a two-level system is often called a *particle detector*<sup>1</sup> in the UDW model, and an *emitter* in the (R)SB model; we will use them interchangeably.

Here we will first revisit the problem of entanglement generation between two UDW detectors interacting with the vacuum state of the non-interacting scalar field, and then initiate the study of tripartite entanglement generation in this model. We are particularly interested in nonperturbative results by going into the *pure dephasing regime*, i.e., when the interaction Hamiltonian commutes with the detectors' free Hamiltonian [27]. The special case of this is when the detectors are *gapless*, which has been studied in the UDW framework in the context of entanglement harvesting and relativistic communication [20, 22, 26, 36, 37]. We will, however, do this using the

closed-system RSB formulation following [29] for several reasons: it gives us a basis for controlling the ultraviolet/infrared (UV/IR) regularity of the model, it is easier to interpret some of the results we present regarding the causal behaviour of the model, and it follows more closely the standard practice in quantum optics. We note that while the dynamics of the pure dephasing regime and the gapless regime are the same, the kinematics are different: for example, gapless RSB model has degenerate joint ground states [29–32].

More specifically, we use the non-perturbative RSB model to study how the entanglement generated between two and three initially uncorrelated detectors via local interactions with the field depends its wave properties dictated by the *strong Huygens principle*, which governs the support of the Green's functions of the wave equation [38–40]. There are primarily two reasons that motivate our analysis. First, on the one hand there is a no-go theorem forbidding entanglement extraction from the vacuum in the gapless model if the detectors' interaction regions are spacelike-separated [22], while for massless field in (3+1)D Minkowski spacetime two detectors can be entangled (as expected) if we allow for causal contact [37]. On the other hand, perturbatively the maximal entanglement occurs at the light cone [41] as it is enhanced by signalling, which in turn depends on the strong Huygens principle. Second, we would like to study the tripartite entanglement scenario, which has been done for a closely related *delta-coupled* variant [28, 42, 43], as this will inform us of the extent the gapless model is useful for studying multipartite entanglement in the context of QFT in curved spacetimes. These will in turn close the (remaining) gap in the literature for gapless UDW model.

In this work, we show that (i) (highly) entangled states of the two emitters require interactions *very deep* into the light cone — the *entanglement cone* marking the boundary for nonzero entanglement is deeper in the light cone

\* gallockyoshimura@biom.t.u-tokyo.ac.jp

† erickson.tjoa@mpq.mpg.de

<sup>1</sup> This is motivated by Unruh and Hawking effects, as particle number is observer-dependent [1, 3, 33–35].

interior with increasing mass and spacetime dimension; (ii) the mass of the field can generically improve the entanglement generation, at the expense of longer interaction time; we argue, however, that this improvement is somewhat independent of the strong Huygens principle; (iii) unlike the bipartite case where it is possible to generate close to maximally entangled states via the spin-boson interactions, the generation of genuine tripartite entanglement is non-perturbatively hard even at sufficiently long times without any aid from entanglement distillation protocols. Result (iii), in particular, suggests that probing the multipartite entanglement of a relativistic quantum field non-perturbatively via localized probes requires either different probe-based techniques or variants of the UDW model.

This work is organized as follows. In Section II we briefly sketch the setup and establish notation. In Section III we discuss the entanglement dynamics for two detectors/emitters and state some UV/IR regularity requirements for the RSB model. In Section IV we discuss the entanglement dynamics for three detectors/emitters. To ensure that the focus is on the entanglement dynamics, we relegate the remaining technical details regarding the UV/IR regularity of the RSB model to the Appendix A. We adopt the convention that  $c = \hbar = 1$  and use mostly plus signature for the metric. The symbol  $x$  denotes a spacetime event.

## II. SETUP

In this section, we briefly cover the basic ingredients involved in our analysis. We will first briefly review scalar field theory in the algebraic quantum field theory (AQFT), the formulation of UDW model as a closed-system RSB model, and the strong Huygens principle. In order to focus on the physics, we will only cover the bare minimum required to follow this work. The readers can find much more detailed mathematical construction in the following references: for AQFT, we mainly rely on a very accessible exposition of the scalar field theory in [44] (see also [45–47]), while for the UDW model we summarize the exposition in [29], which is essentially inspired by [31, 32].

### A. Scalar field theory in curved spacetime

The starting point is the equation of motion for a real scalar field in an  $(n+1)$ -dimensional globally hyperbolic Lorentzian spacetime  $(\mathcal{M}, g)$  where  $g$  is the metric tensor. We have the Klein-Gordon equation

$$P\phi := (-\square + m^2 + \xi R)\phi(x) = 0, \quad (1)$$

where  $\square = \nabla_a \nabla^a$  is the d'Alembert operator,  $m$  is the mass parameter of the field,  $R$  is the Ricci scalar curvature and  $\xi \geq 0$  quantifies the degree of non-minimal cou-

pling to gravity. Global hyperbolicity and the nature of the Klein-Gordon differential operator  $P$  guarantee that the initial value problem for (1) is well-posed and the spacetime admits a foliation of the form  $\mathcal{M} = \mathbb{R} \times \Sigma$ , where  $\Sigma$  is any Cauchy surface that serves as a constant-time slice. For example, we can foliate Minkowski spacetime, the simplest spacetime with zero curvature, in terms of constant- $t$  spacelike hypersurfaces where  $t$  is the usual inertial time coordinate.

As a hyperbolic differential operator,  $P$  admits unique *advanced and retarded propagators*  $E_A(x, x') = E_R(x', x)$ : they are Green's functions for  $P$  where  $E_R(x, y)$  [resp.  $E_A(x, y)$ ] vanishes if  $x$  is not contained in the causal future (past) of  $y$ . We can then define the so-called *causal propagator*<sup>2</sup>

$$E(x, y) := E_R(x, y) - E_A(x, y), \quad (2)$$

which is now a kernel of  $P$ . The causal propagator is important as it appears in the covariant canonical commutation relation (CCR) of the quantized scalar field:

$$[\hat{\phi}(x), \hat{\phi}(y)] = iE(x, y)\mathbb{1}, \quad (3)$$

where  $\mathbb{1}$  is the identity operator.  $E(x, y)$  is a (bi-)distribution since  $\hat{\phi}(x)$  is an *operator-valued distribution*, i.e., it is only a valid operator acting on some Hilbert space after smearing with some appropriate test function  $f$ . The mathematical formulation based on AQFT thus defines the *smearing field operator*

$$\hat{\phi}(f) := \int_{\mathcal{M}} dV f(x) \hat{\phi}(x), \quad (4)$$

where  $dV = \sqrt{-\det g} d^n \mathbf{x}$  is the invariant volume element and  $f \in C_0^\infty(\mathcal{M})$  is a smooth compactly supported function on  $\mathcal{M}$ . Sometimes the spacetime smearing function  $f$  is interpreted as a localization region of the operator, which reflects our inability to resolve a single point in spacetime.

Within the AQFT framework, the quantized scalar field theory is specified by an *algebra of observables*  $\mathcal{A}(\mathcal{M})$  and a *state*  $\omega$ . The algebra of observables  $\mathcal{A}(\mathcal{M})$  is formally defined as a unital  $*$ -algebra of all possible sums and products of smeared field operators  $\hat{\phi}(f)$  for all possible test functions  $f$  and their adjoints satisfying the smeared CCR

$$[\hat{\phi}(f), \hat{\phi}(g)] = iE(f, g)\mathbb{1}, \quad \forall f, g \in C_0^\infty(\mathcal{M}) \quad (5)$$

<sup>2</sup> In [29] it was clarified how the various conventions of the Green's functions lead to different conventions of the causal propagator, and they can be somewhat confusing. This is because these variations are not fixed solely by the metric signature. Fortunately, in most practical calculations, it does not really matter, as they only affect the overall minus sign that one can typically track. Here we follow [44], which seems to be one of the cleanest.

where

$$E(f, g) = \int_{\mathcal{M} \times \mathcal{M}} dV dV' f(x) E(x, x') g(x'). \quad (6)$$

The Klein-Gordon equation is enforced by the requirement that  $\hat{\phi}(f) = 0$  whenever  $f = Ph$  for some  $h \in C_0^\infty(\mathcal{M})$ . Note that the properties of the Green functions guarantee that  $E(f, g) = 0$  whenever  $f, g$  have spacelike supports. For real scalar fields, this imposes that the generators of  $\mathcal{A}(\mathcal{M})$  are smeared field operators with real test functions.

In order to do physics, we need to specify states in addition to observables. A state is a  $\mathbb{C}$ -linear functional  $\omega : \mathcal{A}(\mathcal{M}) \rightarrow \mathbb{C}$  satisfying positivity  $\omega(A^\dagger A) \geq 0$  and normalization  $\omega(\mathbb{1}) = 1$  for  $A \in \mathcal{A}(\mathcal{M})$ , i.e., it is a map that takes in an observable  $A$  as an input and outputs its expectation value  $\omega(A)$ . Through the Gelfand-Naimark-Segal (GNS) reconstruction theorem, we can obtain the Hilbert space representation of the theory, with the GNS vector  $|\Omega_\omega\rangle$  identified as the “vacuum state” of the theory, and expectation values are given by  $\omega(A) = \langle \Omega_\omega | \pi_\omega(A) | \Omega_\omega \rangle$ . Here  $\pi_\omega : \mathcal{A}(\mathcal{M}) \rightarrow L(\mathcal{H}_\omega)$  is a GNS representation such that  $A$  is represented as a linear operator  $\pi_\omega(A) \in L(\mathcal{H}_\omega)$  acting on a (dense subset of) the GNS Hilbert space  $\mathcal{H}_\omega$ . The main advantage of the AQFT framework is that it treats all Hilbert space representations democratically, as there are infinitely many unitarily inequivalent representations of the CCR algebra [44–47], a feature that is important for studying physical systems that are directly defined in the thermodynamic limit [48]. Indeed, the spin-boson model has been studied in the algebraic framework for the same reason [30–32, 49, 50].

For physical applications, not all states are physically relevant. First, in a relativistic context, we need the states to be *Hadamard states* [51–53]. Concretely, in  $(3+1)$ -dimensional spacetimes, this corresponds to the states whose Wightman two-point functions have the correct “short-distance (UV) behaviour” and they take the form

$$W(x, y) \sim \frac{u(x, y)}{\sigma(x, y)} + v(x, y) \log(\sigma(x, y)) + w(x, y), \quad (7)$$

where  $u, v, w$  are smooth functions, and  $\sigma(x, y)$  is *Synge’s world function*, defined as half the squared geodesic distance between  $x, y \in \mathcal{M}$  with respect to the spacetime metric  $g$ . Eq. (7) should be viewed as a (bi-)distribution, where the first two terms in (7) only depend on the metric and Klein-Gordon equation, and the state dependence only influences the UV-finite, regular part  $w$ .

Second, we need the GNS Hilbert space  $\mathcal{H}_\omega$  to be separable: this is *a priori* not guaranteed (see, e.g., [54] for an explicit example in quantum spin chains in the thermodynamic limit). If we restrict, however, to a subclass of Hadamard states that are *quasifree* (Gaussian), i.e., those whose Wightman  $n$ -point functions are fully specified by their 1- and 2-point functions via Wick’s theorem,

then the resulting quasifree representations give rise to Fock space  $\mathcal{H}_\omega = \mathfrak{F}(\mathcal{H})$  (which is separable), where  $\mathcal{H}$  [44–47] is the so-called *one-particle Hilbert space* associated with the positive-frequency solutions  $\varphi_1, \varphi_2$  of the Klein-Gordon equation with Klein-Gordon inner product

$$\langle \varphi_1, \varphi_2 \rangle_{\text{KG}} = i \int_{\Sigma_t} d\Sigma^a \varphi_1 \nabla_a \varphi_2^* - \varphi_2 \nabla_a \varphi_1^*. \quad (8)$$

Following this construction outlined in [23, 27, 29, 45–47], we recover the standard Fock space construction in canonical quantization, where we can write the field operator in terms of the Fourier mode decomposition

$$\hat{\phi}(x) = \int_{\mathbb{R}^n} d^n \mathbf{k} \hat{a}_\mathbf{k} u_\mathbf{k}(x) + \hat{a}_\mathbf{k}^\dagger u_\mathbf{k}^*(x), \quad (9)$$

where  $u_\mathbf{k}(x)$  (resp.  $u_\mathbf{k}^*$ ) are delta-normalized eigenbasis of the one-particle Hilbert space  $\mathcal{H}$  (resp. conjugate Hilbert space  $\bar{\mathcal{H}}$ )<sup>3</sup> called the *positive (resp. negative) frequency modes*. These modes satisfy the Klein-Gordon equation (1) and they are delta-normalized with respect to the Klein-Gordon inner product

$$\begin{aligned} \langle u_\mathbf{k}, u_{\mathbf{k}'} \rangle_{\text{KG}} &= \delta^n(\mathbf{k} - \mathbf{k}'), \\ \langle u_\mathbf{k}^*, u_{\mathbf{k}'}^* \rangle_{\text{KG}} &= -\delta^n(\mathbf{k} - \mathbf{k}'), \\ \langle u_\mathbf{k}, u_{\mathbf{k}'}^* \rangle_{\text{KG}} &= 0, \end{aligned} \quad (10)$$

and the creation and annihilation operators obey the CCR  $[\hat{a}_\mathbf{k}, \hat{a}_{\mathbf{k}'}^\dagger] = \delta^n(\mathbf{k} - \mathbf{k}') \mathbb{1}$ . The Fock vacuum state of the theory, associated with the GNS vector, is conventionally denoted as  $|0\rangle$  and satisfies the distributional equality  $\hat{a}_\mathbf{k} |0\rangle = 0$  for all  $\mathbf{k}$ . All other states with finite particle number can then be built from applications of (smeared) creation operators on the vacuum state and taking linear combinations.

For many practical computations and in order to avoid domain issues associated with unbounded operators  $\hat{\phi}(f)$ , it is often convenient to work instead with the so-called *Weyl algebra*  $\mathcal{W}(\mathcal{M})$ , which is formally an exponentiated version of the field operator, i.e., it is a  $C^*$ -algebra generated by objects of the form  $e^{i\phi(f)}$  (see [45] for more details). One can then find the corresponding state whose GNS construction gives the same physical theory, with the GNS representation  $\Pi_\omega : \mathcal{W}(\mathcal{M}) \rightarrow \mathcal{B}(\mathcal{H}_\omega)$  related via derivatives.<sup>4</sup> We note that the state  $\omega$  is completely specified by its Wightman  $n$ -point function:

$$W(f_1, \dots, f_n) := \omega(\hat{\phi}(f_1) \dots \hat{\phi}(f_n)). \quad (11)$$

<sup>3</sup> The one-particle Hilbert space is related to the (complexified) solution space of (1)  $\text{Sol}_\mathbb{C}(\mathcal{M})$  via  $\text{Sol}_\mathbb{C}(\mathcal{M}) = \mathcal{H} \oplus \bar{\mathcal{H}}$ , i.e., all complex solutions are linear combinations of positive and negative frequency modes.

<sup>4</sup> Strictly speaking, the states used for  $\mathcal{A}(\mathcal{M})$  and  $\mathcal{W}(\mathcal{M})$  are not the same, but there is a bijection between them [55].

For our purposes, it is useful to write

$$\hat{\phi}(f) = \hat{a}(f_{\mathbf{k}}^*) + \hat{a}^\dagger(f_{\mathbf{k}}) \equiv \hat{\phi}(f_{\mathbf{k}}), \quad (12)$$

where

$$\hat{a}(f_{\mathbf{k}}^*) = \int_{\mathbb{R}^n} d^n \mathbf{k} \hat{a}_{\mathbf{k}} f_{\mathbf{k}}^*, \quad f_{\mathbf{k}} = \int_{\mathcal{M}} dV f(\mathbf{x}) u_{\mathbf{k}}^*(\mathbf{x}). \quad (13)$$

This relabeling is useful as it emphasizes which of the field modes we are accessing by choosing a particular space-time smearing function  $f$ . This “momentum space” representation of the field operators will be used often for the rest of this work. In Minkowski space, we note that the mode functions are exactly known, and thus they serve as examples where calculations can be done explicitly: in the standard inertial coordinates  $(t, \mathbf{x})$ , we have

$$u_{\mathbf{k}}(t, \mathbf{x}) = \frac{1}{\sqrt{2(2\pi)^n \omega_{\mathbf{k}}}} e^{-i\omega_{\mathbf{k}} t + i\mathbf{k} \cdot \mathbf{x}}, \quad (14)$$

where  $\omega_{\mathbf{k}}^2 = |\mathbf{k}|^2 + m^2$  is the relativistic dispersion relation.

## B. UDW model as a time-independent RSB model

The setup we have in mind involves two UDW detectors or emitters A and B interacting locally with a relativistic scalar field. Let us recall the standard prescription based on the covariant formulation of the original UDW model in terms of the Hamiltonian density in the interaction picture [9].

In the original UDW framework, we first assume that the center of mass (COM) of each detector follows a time-like trajectory  $\mathbf{z}_j(\tau_j)$ ,  $j \in \{A, B\}$ , parametrized by their own proper time  $\tau_j$ , and then in the COM frame we establish the so-called Fermi normal coordinates (FNC) adapted to the trajectory  $\bar{\mathbf{x}} \equiv (\tau, \bar{\mathbf{x}})$  where the COM trajectory is parametrized by  $\mathbf{z}_j(\tau_j) \equiv (\tau_j, \bar{\mathbf{0}})$  [56]. The point of setting up an FNC is to be able to make a physically reasonable assumption that the interaction between the detector and the field is specified by the spacetime smearing of the form  $f(\mathbf{x}(\bar{\mathbf{x}})) = \chi(\tau) F(\bar{\mathbf{x}})$ , i.e., in the rest frame of the detector we can tell apart the spatial profile  $F(\bar{\mathbf{x}})$  (associated with, say, atomic orbitals of an atom) from the *switching function*  $\chi(\tau)$  that determines the duration and strength of the interaction. This implicitly assumes that the spatial profile is time-independent within the rest-frame, i.e., we are working in a regime where the detector is (Born-)rigid. The interaction Hamiltonian density in the interaction picture thus takes the form

$$\hat{h}_I^{(j)}(\bar{\mathbf{x}}) = \lambda_j f^{(j)}(\tau, \bar{\mathbf{x}}) \hat{O}_j(\tau) \otimes \hat{\phi}(\mathbf{x}(\tau, \bar{\mathbf{x}})), \quad (15)$$

where  $j = A, B$ ,  $\lambda_j \geq 0$  is the coupling constant and  $\hat{O}_j$  is some detector observable. We can then compute the unitary operator generated by this Hamiltonian in the

interaction picture, namely

$$\hat{U}_I = \mathcal{T}_t \exp \left[ -i \int_{\mathcal{M}} dV \hat{h}_I^{(A)}(\mathbf{x}) + \hat{h}_I^{(B)}(\mathbf{x}) \right], \quad (16)$$

where  $\mathcal{T}_t$  is a time-ordering symbol with respect to some global time function. In most cases, one has to perform a perturbative Dyson series truncation, and even then it is mostly intractable except in special cases, such as (conformally) flat spacetimes and specific trajectories, unless one takes a specific limit where the unitary operator above can be calculated exactly — this happens for the so-called delta-coupling and pure-dephasing models [19–28].

As argued in [29], the UDW model has the nice property that its interaction can be made strictly local in spacetime, so that two detectors A and B can be said to be spacelike separated or not by checking the supports of their interaction profiles  $f^{(j)}$ . This support property is often taken to represent the portion of spacetime operationally accessible to the corresponding observer, although the algebra of observables that the observer can effectively access can be strictly larger than the interaction region.<sup>5</sup> Taking this difference into account, we can instead reframe the UDW model in the spirit of standard quantum optics, which goes by the name of *spin-boson (SB) models*. Traditionally, the SB model is defined in flat spacetime and directly in the momentum representation: for a single two-level emitter, its Hamiltonian reads

$$\hat{H} = \frac{\Omega}{2} \hat{\sigma}_z + \Delta \hat{\sigma}_x + \int_{\mathbb{R}^n} d^n \mathbf{k} \omega_{\mathbf{k}} \hat{a}_{\mathbf{k}}^\dagger \hat{a}_{\mathbf{k}} + \hat{\sigma}_x \otimes \int_{\mathbb{R}^n} d^n \mathbf{k} \left( \hat{a}_{\mathbf{k}} F_{\mathbf{k}}^* + \hat{a}_{\mathbf{k}}^\dagger F_{\mathbf{k}} \right), \quad (17)$$

where  $\Omega$  is the energy gap,  $\Delta$  measures the shift due to the detector’s internal “magnetic” response, the third term is the field’s free Hamiltonian, and  $F_{\mathbf{k}}$  is called the *coupling function* that prescribes which modes the detector couples to and by how much. By construction, this model is *time-independent* as the coupling functions are not dependent on time. We can think of this as a “closed system” formulation of the UDW model where we model the interaction to be always on. Despite this constant-switching interaction, the spacetime locality of observers are still well-defined in the sense that the support of the interaction is localized in space, while the observables accessible to each observer are localized in space and time. Reformulating the UDW model in terms of the constant-switching SB Hamiltonian in (17) we have

$$\hat{H}_{\Omega, \Delta, \lambda} = \sum_j \hat{H}_0^{(j)} + \hat{H}_{\phi, 0} + \sum_j \hat{H}_{\text{int}}^{(j)}, \quad (18)$$

<sup>5</sup> For example, a pointlike detector has interaction profile  $f$  supported only along its timelike trajectory, but the accessible algebra of observables is prescribed by its *timelike envelope*, the smallest causal diamond containing  $\text{supp } f$ .

where  $\hat{H}_0^{(j)}$  and  $\hat{H}_{\phi,0}$  are the free Hamiltonians for detector- $j$  and the field, respectively, and  $\hat{H}_{\text{int}}^{(j)}$  is the interaction Hamiltonian that couples detector- $j$  and the field. These are explicitly written as

$$\hat{H}_0^{(j)} = \frac{\Omega_j}{2} \hat{\sigma}_z^{(j)} + \Delta_j \hat{\sigma}_x^{(j)}, \quad (19a)$$

$$\hat{H}_{\phi,0} = \int_{\mathbb{R}^n} d^n \mathbf{k} \omega_{\mathbf{k}} \hat{a}_{\mathbf{k}}^\dagger \hat{a}_{\mathbf{k}} \quad (19b)$$

$$\hat{H}_{\text{int}}^{(j)} = \hat{\sigma}_x^{(j)} \otimes \int_{\mathbb{R}^n} d^n \mathbf{k} \left( \hat{a}_{\mathbf{k}} F_{\mathbf{k}}^{(j)*} + \hat{a}_{\mathbf{k}}^\dagger F_{\mathbf{k}}^{(j)} \right), \quad (19c)$$

where

$$F_{\mathbf{k}}^{(j)} = \lambda_j \int_{\Sigma_\tau} d\Sigma_\tau F^{(j)}(\bar{\mathbf{x}}) u_{\mathbf{k}}^*(0, \mathbf{x}(\bar{\mathbf{x}})), \quad (20)$$

with respect to some foliation associated with constant- $\tau$  surfaces. Note that the coupling constants are dimensional as  $[\lambda_j] = [\text{Length}]^{(n-3)/2}$  in  $(n+1)$ -dimensional spacetime.

For convenience, we will distinguish the original UDW model described by the Hamiltonian (15) from our time-independent, SB-type formulation in (18) by calling the latter the relativistic spin-boson (RSB) model. This terminology can be understood from the idea that in momentum space, what distinguishes the model from a generic SB model is the relativistic dispersion.

There are obvious limitations to this formulation that the original UDW model (15) does not have [29]. As currently stated, it only works for *static trajectories* with respect to the quantization frame, as otherwise  $F_{\mathbf{k}}^{(j)}$  in Eq. (20) would be time-dependent, which would correspond to time-dependent coupling (as is the case for Unruh effect or adiabatic switching). It follows that, for multiple detectors, all COM trajectories are static relative to one another, and must align with the Killing vector field generating time translations of the spacetime. Consequently, the SB framework with a time-independent Hamiltonian by default excludes some of the natural settings where the usual UDW approach thrives, e.g., the analysis of relative motion or accelerating trajectories. We will not discuss how to handle these issues in this work, and we refer to [57] for how this is handled in the case of the Unruh effect.

These limitations notwithstanding, we name two reasons why the RSB formulation is relevant for us.

(a) It allows for a rigorous treatment of the model, i.e., whether it has good UV and IR properties. For example, in the single-emitter case, the existence of ground states of the model depends on the UV/IR regularity of the coupling function  $F_{\mathbf{k}}$  [30–32]. In the UDW language, this corresponds to making an appropriate choice of spatial smearing  $F(\mathbf{x})$ , whose properties are tied to the Klein-Gordon equation and

the spacetime dimension [29].<sup>6</sup> There have been a few nice developments providing rigorous studies of the thermalization of an Unruh-DeWitt detector in the weak-coupling regime [57, 62, 63].

(b) It allows for analysis of relativistic causality in a manner closer to the standard quantum optics. For example, it is much simpler to specify how long the interaction has to occur before the detectors can effectively signal to one another by checking that  $t \gtrsim L$ , where  $L$  is the separation of their COM. This is particularly useful for one of our results, where we will show that significant entanglement is only generated “deep in the light cone interior” (*c.f.* Section III).

For completeness, we will extend the regularity requirements for single detectors in [29] to  $N$  detector settings. These will be relevant for a better understanding of how the entanglement dynamics of the two initially separable detectors depend on the mass of the field and the spacetime dimensions. This goes by the name *strong Huygens principle*, which we briefly discuss below.

### C. Strong Huygens principle

One of our goals is to understand the impact of the mass and spacetime dimensions on the entanglement dynamics between two detectors in the non-perturbative regime, since these modify the signaling contribution to the dynamics. The perturbative analysis has been covered in the literature [41, 64, 65].

Roughly speaking, a field  $\phi$  is said to satisfy the strong Huygens principle when its Green’s function has distributional support only on the light cone [38]. Intuitively, this means that an impulsive light emanated from an emitter can be captured only by a lightlike separated receiver. When support extends inside the light cone, we say the strong Huygens principle is violated, and a signal can be captured by a timelike receiver. By construction, massive fields violate the strong Huygens principle as massive excitations travel at subluminal speed. The simplest example of the strong Huygens principle is the massless scalar field in  $(3+1)$ -dimensional Minkowski spacetime, where in the inertial coordinates the causal propagator is given by

$$E(\mathbf{x}, \mathbf{x}') = \frac{\delta(t - t' + |\mathbf{x} - \mathbf{x}'|) - \delta(t - t' - |\mathbf{x} - \mathbf{x}'|)}{4\pi|\mathbf{x} - \mathbf{x}'|} \quad (21)$$

<sup>6</sup> In the UDW framework, it is often the case that Gaussian smearing is used for calculational convenience, but its non-compact support leads to mild and quantifiable degrees of causality violation in these models [58–61]. Provided the detectors are not pointlike, spatial smearings often grant good UV regularity; what remains is to check that the model is also IR regular.

Clearly, the field obeys the strong Huygens principle by virtue of the fact that the Dirac delta function has no support except when  $\Delta t = \pm|\Delta\mathbf{x}|$ , i.e., two points are null-separated. It is also known that in  $(n+1)$ -dimensional flat spacetime, the wave equation  $\square\phi = 0$  fails the strong Huygens principle for odd spacetime dimension ( $n$  even) and when  $n = 1, 2$ . In even spacetime dimensions the strong Huygens principle is satisfied (see [41, 58] for some explicit computations).

Remarkably, some generic results about the violation of the strong Huygens principle can be obtained for curved spacetimes [39, 40]. Some intuition can be gleaned from the Klein-Gordon equation in (1): if we consider a generic non-minimal coupling parameter  $\xi > 0$ , then massless fields coupled to gravity acquire effective mass due to the Ricci scalar contribution. Indeed, for constant-curvature geometry, this effectively gives a mass parameter  $m_{\text{eff}} := \sqrt{\xi R}$ , so the Klein-Gordon equation is equivalent to that of a massive field minimally coupled to gravity ( $\xi = 0$ ). The importance of the strong Huygens principle is that it affects the propagation of information: indeed, massless fields that violate the strong Huygens principle can signal to the *interior* of the light cone as the Green's function between two timelike-separated events is non-vanishing. The violation of the strong Huygens principle has been shown, using perturbative techniques, to impact how two UDW detectors can be entangled when they are in causal contact [41, 64] and how they can be exploited to send timelike signals using massless fields [66, 67].

#### D. Regularity conditions

Before we proceed with analysis of the bipartite entanglement dynamics, we first take a detour to establish some regularity requirements for the RSB model for  $N$ -emitters. This will justify in part the use of our model instead of the usual interaction picture, and also why it will be useful to work with covariant IR-cutoff  $m \ll 1$  (in an appropriate unit) for dealing with massless case. Readers interested only in the physical results pertaining entanglement dynamics of the two detectors can skip to Subsection III. In order to keep the discussion fairly accessible, we will try to frame our results in rigorous terms but with fairly physicist-angled explanation.

The first assumption we will make is the following:

**Assumption 1** (pure-dephasing and no zero mode). *The RSB model is chosen to be pure-dephasing, i.e., with energy gap  $\Omega_j = 0$ , such that the interaction Hamiltonian (19c) commutes with the free qubit Hamiltonians  $\hat{H}_0^{(j)} = \Delta_j \hat{\sigma}_x^{(j)}$ , i.e.,*

$$[\hat{H}_{\text{int}}^{(i)}, \hat{H}_0^{(j)}] = 0, \quad \forall i, j \in \{A, B, C, \dots\}. \quad (22)$$

*Furthermore, we will assume that the background spacetime is such that the Hilbert space representation admits*

*no zero modes.*

By ‘zero mode’ we mean the field mode that is not associated with the 1-particle sector of the Fock space, i.e., it behaves like a free particle in quantum mechanics [46, 68–70] and hence does not admit a Fock representation. This complicates the choice of the vacuum state on which the full Hilbert space can be built (see, e.g., [68, 69] for simple examples on Einstein cylinder), so we will avoid them for simplicity as they can be dealt only case-by-case.

Although it is not useful for studying weakly-coupling phenomenon such as the Unruh effect, the pure-dephasing regime in Assumption 1 is important as they can still exhibit rich dynamics and they enable rigorous results. More technically, the pure-dephasing model can be viewed as a  $C^*$ -dynamical system, which roughly speaking means that the dynamics can be implemented by an automorphism  $\alpha_t^0 : \mathcal{A} \rightarrow \mathcal{A}$  where  $\mathcal{A}$  is the *joint algebra of observables* of the detector-field system, independently of the Hilbert space representations. This is to be contrasted with the nonzero gap case, where the corresponding automorphism can only be rigorously defined as a *pseudodynamics* [48], i.e., one has to work with an implementation of  $\alpha_t^\Omega : \mathcal{B}(\mathcal{H}_\omega) \rightarrow \mathcal{B}(\mathcal{H}_\omega)$  in a particular Hilbert space representation. Morally speaking, this is due to the fact that for  $\Omega \neq 0$ , there is no guarantee that  $\alpha_t^\Omega$  will not “bring us outside the Hilbert space” and give rise to divergences. The best one can do is to do a “small  $\Omega$ ” perturbative calculation about the pure-dephasing as the perturbation is bounded [31]. Treating the interaction Hamiltonian as a perturbation to the free Hamiltonian is much harder due to unbounded nature of the field operator (see, e.g., [49, 50]).

Apart from the issue of mathematical rigor, the main physical reason for choosing Assumption 1 is for the sake of having rigorous results even for the strong coupling regime where the coupling constants  $\lambda_j$  for each detector can be chosen to be arbitrarily large. In the original UDW case, it was shown that if the interaction Hamiltonian of the UDW model (15) has spacelike supports, then the reduced density matrix of the two detectors after interaction is separable [22]. The key, of course, is spacelike separation as we know that generic interacting quantum systems that are in causal contact will generate some entanglement, and the same gapless model was shown to generate entanglement when they are in causal contact [37].

As we will show in Section III, one of our contribution will be to show that not only does the RSB model satisfy the no-go theorem, but that the detectors can only get entangled *very deep into the light cone*. In other words, even though we can in principle make the final state arbitrarily close to the maximally entangled state, it takes much longer than the light-crossing time between them. To set up the stage for these results, we need more assumptions along the lines used for the single detector case in [29]. These additional assumptions require us to first study the ground state properties of the full detector-field

system.

The first result is to guarantee that the ground state energy is bounded from below, assuming the existence of a ground state from the GNS construction.<sup>7</sup>

**Proposition 1.** *Consider  $N$  detectors,  $A, B, \dots$ , described by the RSB Hamiltonian (18) in  $(n + 1)$ -dimensional spacetime. Then, for gapless detectors  $\Omega_j = 0$ , the expectation value of the Hamiltonian  $\langle \hat{H}_{0,\Delta,\lambda} \rangle$  has a lower bound given by*

$$\langle \hat{H}_{0,\Delta,\lambda} \rangle \geq \mathbf{s} \cdot \mathbf{\Delta} - R_1(\mathbf{s} \cdot \mathbf{F}_{\mathbf{k}}, n), \quad (23)$$

for some choice of  $\mathbf{s} \in \{\pm 1\}^N$ , where  $\mathbf{\Delta} = [\Delta_A, \Delta_B, \dots]^\top$  and  $\mathbf{F}_{\mathbf{k}} = [F_{\mathbf{k}}^{(A)}, F_{\mathbf{k}}^{(B)}, \dots]^\top$  are the  $N$ -dimensional vectors dependent on  $\Delta_j$  and the coupling functions, respectively, and

$$R_\alpha(f_{\mathbf{k}}, n) := \int_{\mathbb{R}^n} \frac{d^n \mathbf{k}}{\omega_{\mathbf{k}}^\alpha} |f_{\mathbf{k}}|^2, \quad \alpha \in \mathbb{R}_0^+. \quad (24)$$

Hence, the RSB Hamiltonian is bounded from below if  $R_1(\mathbf{s} \cdot \mathbf{F}_{\mathbf{k}}, n) < \infty$ .

The proof is given in Appendix A for completeness.

Essentially, Proposition 1 can be understood as the fact as follows: by performing appropriate Bogoliubov transformation the joint interacting ground state is essentially a tensor product of the eigenstates of  $\hat{\sigma}_x$  and some (multimode) coherent state of the field whose coherent amplitude depends on the detector-field coupling. The only subtlety is that this argument assumes that the total number of particles in the ground state is finite.

**Proposition 2.** *The joint interacting ground state has a finite particle number if  $R_2(\mathbf{s} \cdot \mathbf{F}_{\mathbf{k}}, n) < \infty$  for all  $\mathbf{s}$ .*

The proof is a simple adaptation of [31] except that we need to consider all choices of signs  $\mathbf{s}$  and that the integral  $R_2$  is with respect to the ‘‘combined smearing function’’  $\mathbf{s} \cdot \mathbf{F}_{\mathbf{k}}$ . In particular, we see that the model exhibits IR divergences (production of an infinite number of soft bosons in the thermodynamic limit) if at least one detector is not coupled to the field with a sufficiently IR-regular coupling function  $F_{\mathbf{k}}^{(j)}$ .

As argued in [29], this suggests that modelling a physical system with the RSB or UDW framework requires careful control of both UV and IR behavior. The UV regularity is automatically taken care of by giving each

detector a finite size (effectively serving as a UV cutoff), but the IR case is more subtle. If the field is massive or gains effective mass through, say, coupling to the (classical) gravitational field, then the model is also IR-regular. In contrast, when there are soft bosons, such as (3+1)-dimensional Minkowski spacetime with massless field, the key insight to be learnt from [30–32, 49, 50] is to consider a different Hilbert space representation that is not unitarily equivalent to the vacuum representation: indeed, the Araki-Woods representation and the thermal KMS representation suffice for the situation at hand [71, 72] (see [62] for very recent analysis on KMS states). At the level of correlation functions, the vacuum correlators can be computed by taking the zero-temperature limit of the thermal correlators.

Since in this work we are going to focus on entanglement dynamics, the situation involving the infinitely many soft boson productions will not be of concern to us. Indeed, perturbatively one can check (following the strategy in [41]) that very light scalar field ( $m \approx 0$ ) leads to bipartite entanglement between the detectors that is indistinguishable compared to the massless case. Thus we are going to assume this:

**Assumption 2.** *The scalar field is assumed to have mass  $m > 0$ . Massless fields will be viewed as having a covariant IR cutoff given by a small but finite mass  $m$ .*

In the context of our results, we will consider the field to be massless for parameter  $m\sigma \ll 10^{-11}$  where  $\sigma$  is the effective size of the detector. Crucially, this implies that the RSB model is both UV- and IR-regular in the sense above, it follows that the non-interacting Hilbert space is unitarily equivalent to the joint interacting Hilbert space, i.e., the interacting Hilbert space is  $\mathbb{C}^2 \otimes \mathbb{C}^2 \otimes \mathfrak{F}(\mathcal{H})$  where  $\mathfrak{F}(\mathcal{H})$  is the Fock space of the free field theory. In the subsequent analyses we will make these assumptions for simplicity, noting that one can always pass to the correct Hilbert space representation when the IR regularity needs to be dropped [29, 31, 32].

### III. ENTANGLEMENT DYNAMICS BETWEEN TWO DETECTORS

In this section, we revisit the scenario of entanglement dynamics between two UDW detectors interacting with a scalar field initialized in the uncorrelated ground state of the non-interacting theory ( $\lambda_j = 0$ )  $|\psi(0)\rangle = |g_A\rangle |g_B\rangle |0\rangle$ . It is instructive to survey the relevant known results for two original UDW detectors, all of which were done in the interaction picture:

- (i) Perturbatively, spacelike-separated detectors with interaction Hamiltonian not commuting with their free Hamiltonian can be entangled starting from initially separable state. This is the well-known entanglement harvesting protocol [73–77], and has been studied extensively in various scenar-

<sup>7</sup> We are following the construction in [31]: there, one assumes first the existence of a ground state in the form of some vector  $|\psi\rangle \in \mathcal{H}_\omega \cong \mathbb{C}^2 \otimes \mathfrak{F}(\mathcal{H})$ , and then find the ground state energy. The inadequacy of this construction comes from the issue of whether  $\mathfrak{F}(\mathcal{H})$  is the *non-interacting Fock space*, in which case one has to construct the state by, e.g., taking zero-temperature limit of some thermal state. From the calculational point of view, it will turn out that the ground state energy will be the same either way as we can just view  $|\psi\rangle$  as a GNS vector.

ios (curved spacetimes, different detector models, etc.).

- (ii) Perturbatively, detectors can be entangled also when the interaction is causally connected [73], however this entanglement can be independent of the vacuum entanglement of the field state depending on the wave property known as the strong Huygens principle [41, 65, 78].
- (iii) Non-perturbatively, it is known that *delta-coupled* detectors cannot get entangled at spacelike separation if it is “simple-generated” [22] (i.e., each detector interacts instantaneously *once* [27]), but can get entangled otherwise.
- (iv) Non-perturbatively, gapless detector models cannot extract entanglement at spacelike separation, based on arguments about entanglement-breaking channels [22, 79]. Consequently, initially separable detector remains separable after interaction.
- (v) Non-perturbatively, it was shown in [37] for massless fields in (3+1)D Minkowski spacetime that gapless models can get entangled if interaction time is long enough for detectors to be in causal contact.<sup>8</sup> This analysis was motivated partially to better understand gravity-induced entanglement setups [82].

There are countless results in the literature involving similar setups but different detector trajectories, boundary conditions, spacetime geometries, initial states, etc. that are only tangentially relevant for our purposes, so we do not aim for an exhaustive list.

Our initial goal is to complement the analysis in the literature concerning (ii), (iv) and (v). That is, we carry out a fully non-perturbative analysis of entanglement dynamics between two gapless detectors that are in causal contact in scenarios where the strong Huygens principle is violated, i.e., accounting for the effects of mass and spacetime dimensions. As we show below, pursuing this goal has a good payoff: it turns out that the entanglement dynamics is actually richer and non-trivial once we include mass and spacetime dimension as tunable parameter.

We first recall that the original interest in the so-called entanglement harvesting protocol is fundamental in nature, since it was to see whether vacuum entanglement can be detected at all [73–77]. For this reason, it is immaterial that the amount of entanglement is extremely small

or whether the calculations are only perturbative in nature, as the main purpose is as a sort of “witness” for vacuum entanglement in the field. From a theoretical standpoint, there is nothing very surprising about the protocol itself: what is non-trivial is whether it is detectable in practice. Several experimental proposals have been given, from the early proposal involving linear ion trap [83] to the recent superconducting circuits [84], with recent experimental realization via electro-optics sampling experiment [85].

On the other hand, if the goal is to generate entanglement, the quality matters and it is somewhat immaterial that the entanglement is extracted from the vacuum of the field (which would be very small in general). Indeed, physical intuition tells us that it is generically unsurprising for two quantum systems A and B to get entangled in general if we allow them to have direct interactions and one has to engineer the interactions and the initial states to avoid getting entangled. The same is true if we allow induced interactions, i.e., the two systems interact with a common third party C that induces effective interactions between the two. Essentially, C mediates the interaction by propagating signals from A to B (it could be phonons, photons, etc.). Consequently, the physically relevant question is how the entanglement is generated and how good it can be as a function of parameters. This necessitates non-perturbative approach, as perturbation theory only allows perturbatively small amount of entanglement.

With the above perspectives in mind, we would like to better understand how entanglement is generated between two initially uncorrelated detectors interacting with the vacuum state of a non-interacting scalar field as a function of time, separation, mass and spacetime dimensions. The RSB gapless model has two advantages over the standard UDW model in that (i) it can be defined rigorously [29–32] and that (ii) the causal relationship can be defined sharply without any (exponential) tails from the original UDW model employing Gaussian (adiabatic) switching. Our results will be presented numerically in what follows. All results are plotted with the detector’s effective size  $\sigma$  as a reference length scale, and we use dimensionless coupling constant  $\tilde{\lambda} \equiv \lambda\sigma^{-(n-3)/2}$ . The initial state of the total system at  $t = 0$  is an uncorrelated state  $|\psi(0)\rangle = |g_A\rangle |g_B\rangle |0\rangle$ , where  $|g_j\rangle$  is the ground state of  $\hat{\sigma}_z^{(j)}$ . Massless fields are taken to be the case when  $m\sigma = 10^{-11}$  (IR-regulated) with numerically verified convergence. We note that nonzero gap ( $\Delta_j \neq 0$ ) does not alter the dynamics at all, so these results apply equally well to generic  $\Delta_j$ . Hence in what follows we set  $\Delta_j = 0$ .

In Fig. 1 we plot the negativity of entanglement  $\mathcal{N}$  as a function of separation  $L$  between the detectors’ center of mass and the duration of interaction  $t$  for the weak coupling regime  $\tilde{\lambda} = 0.01$ , with a) showing the massless regime and b) showing the massive regime. In both massless and massive cases, we see that the UDW-type coupling can be used to generate bipartite states close to

<sup>8</sup> It was also shown in [37] that if the coupling is also sufficiently weak, the two-detector dynamics can be approximated in some sense by an entangling unitary. The latter is essentially the same spirit as the well-known semiclassical optics calculation where the electromagnetic field is not quantized [80, 81].

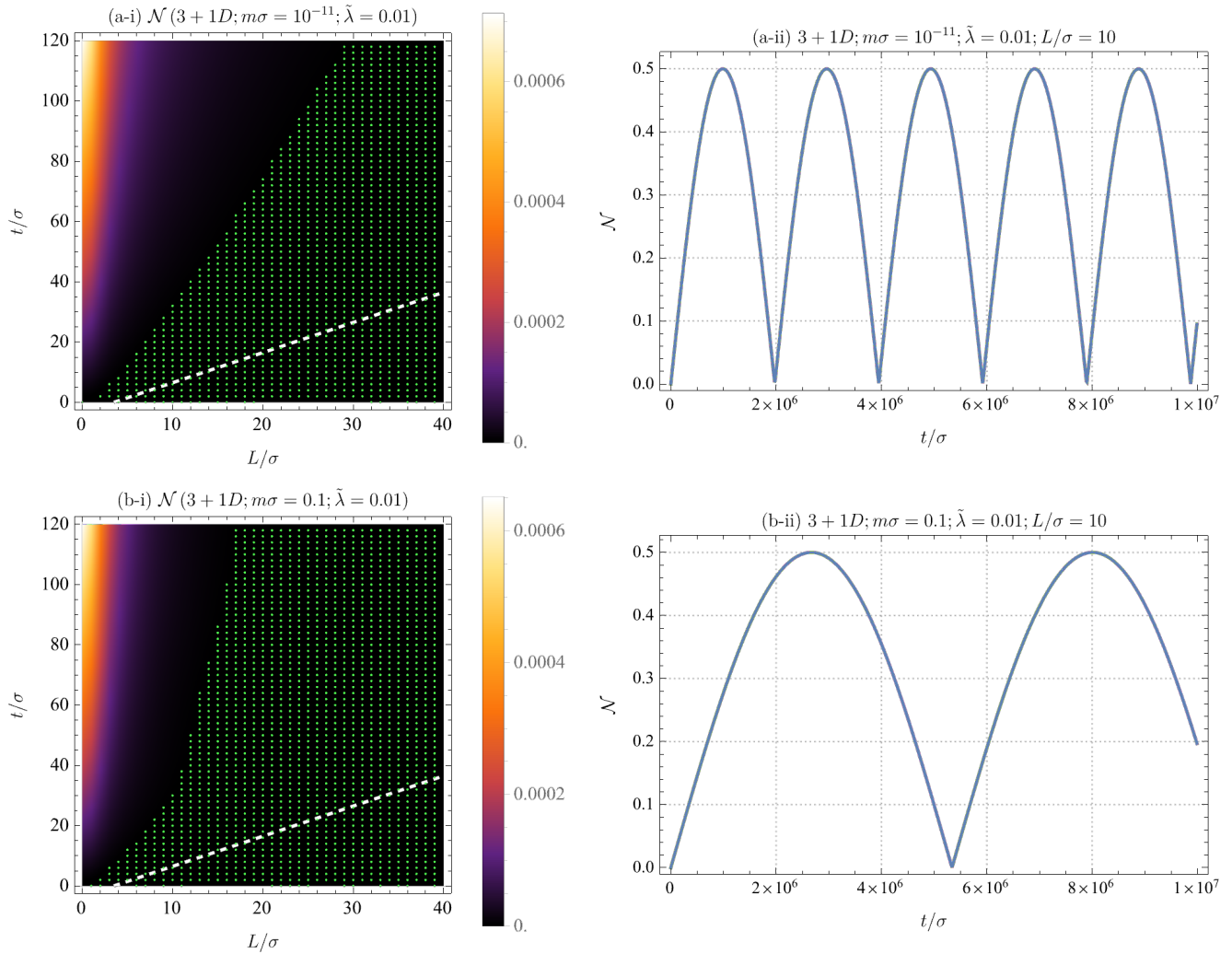


FIG. 1. Density plots [(a-i) and (b-i)] of negativity  $\mathcal{N}$  between two inertial detectors weakly coupled to the field ( $\tilde{\lambda} = 0.01$ ) with  $\Delta_A = \Delta_B = 0$  in (3+1)-dimensional Minkowski spacetime when the mass of the field is (a)  $m\sigma = 10^{-11}$  and (b)  $m\sigma = 0.1$ . The green dots depict the region where  $\mathcal{N} = 0$ , and the white dashed line represents the light cone from the edge of the detector (which starts from  $L/\sigma \approx 3.5$  at  $t = 0$ ), whose COM is located at the origin of the diagrams. On the right-hand side [(a-ii) and (b-ii)], the time dependence of  $\mathcal{N}$  at  $L/\sigma = 10$  is depicted.

being maximally entangled.<sup>9</sup> However, perhaps surprisingly, both Fig. 1a-i) and b-i) show that the light cone (white dashed line) has a much gentler slope than the black boundary which marks the beginning of nonzero entanglement — for convenience we call these “entanglement cone”. In other words, significant amount of entanglement can only be generated *very deep into the light cone*. This is to be contrasted with the standard perturbative result for the UDW model, where entanglement peaks in general *at* the light cone [41]. The entangle-

ment cone is not linear in the  $t - x$  plane, and we see that increasing the mass makes the entanglement cone steeper (i.e., it takes much longer time to reach maximum entanglement).

In Fig. 2 we plot the same scenario in (3+1)D for the strong coupling regime  $\tilde{\lambda} = 1$ . In the strong coupling regime, we observe that the entanglement cone is *unchanged* compared to the weak coupling, however the maximum amount of entanglement is much lower in both massless and massive cases. In fact, we observe that not only does the massless entanglement decay in time, but its maximum is *lower* than that for the massive field. In other words, mass *enhances* the amount of entanglement generated for the two detectors. Note that because the RSB model used here is gapless, this cannot be explained by any resonance-type argument (which works

<sup>9</sup> For the massless case, the fact that we can generate significant amount of entanglement can already be inferred from [37] with suitable adjustment and rescaling (to account, for instance, the Gaussian switching).

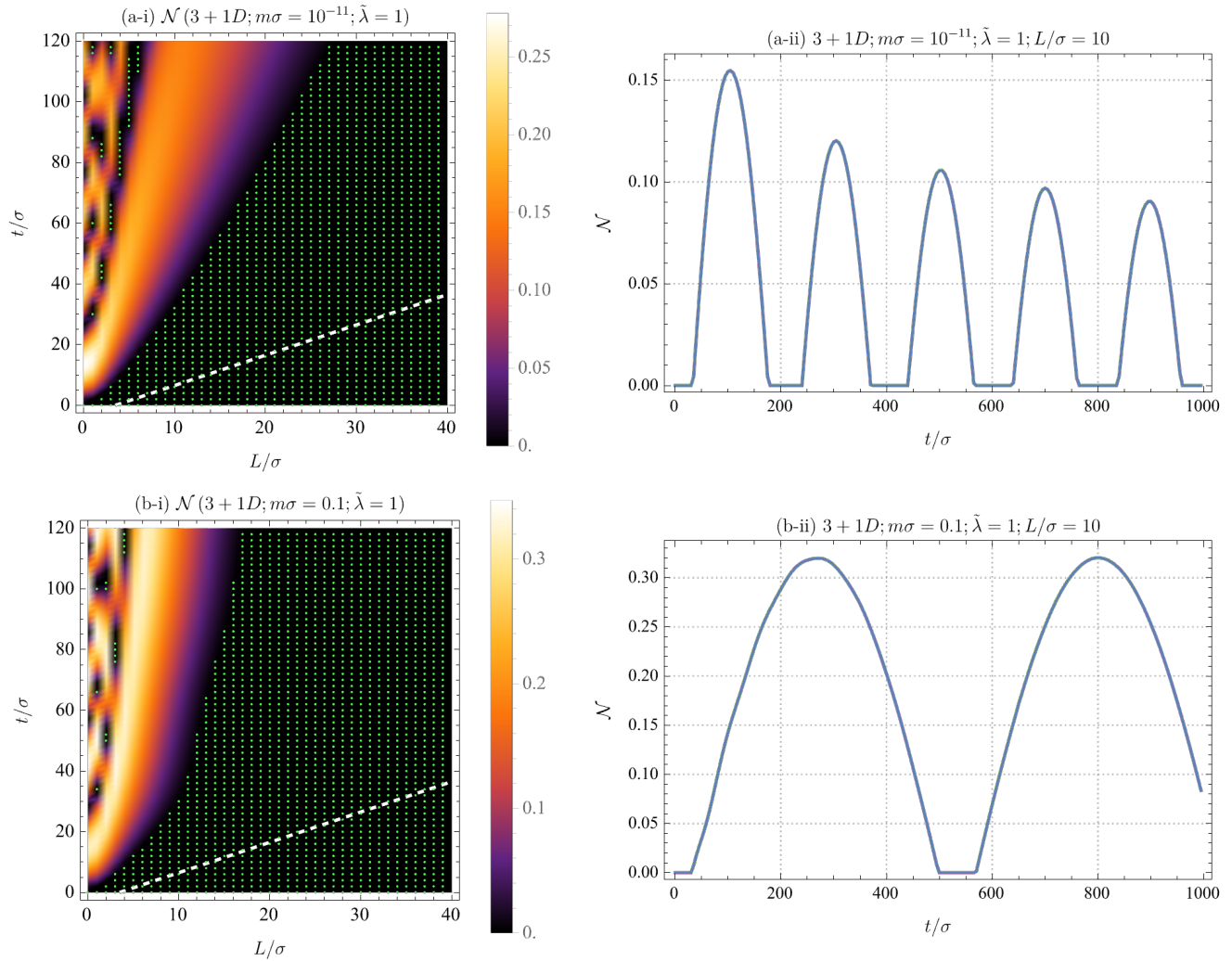


FIG. 2. Density plots [(a-i) and (b-i)] of negativity  $\mathcal{N}$  between two inertial detectors strongly coupled ( $\tilde{\lambda} = 1$ ) to the field in  $(3+1)$ -dimensional Minkowski spacetime when the mass of the field is (a)  $m\sigma = 10^{-11}$  and (b)  $m\sigma = 0.1$ . The green dots depict the region where  $\mathcal{N} = 0$ , and the white dashed line represents the light cone from the edge of the detector (which starts from  $L/\sigma \approx 3.5$  at  $t = 0$ ), whose COM is located at the origin of the diagrams. On the right-hand side [(a-ii) and (b-ii)], the time dependence of  $\mathcal{N}$  at  $L/\sigma = 10$  is depicted.

in the perturbative regime as in [65]). Importantly, this is not contradicting any intuition about “exponential decay” associated with mass: mass contributes to the exponential decay of correlations *as a function of separation*  $L$ , but not as a function of temporal duration  $t$  — this can be checked, for instance, by looking at the asymptotic behaviour of the Wightman two-point functions in the large- $t$  or large- $L$  limit.

At this stage, it is unclear if this phenomenon is tied to the strong Huygens principle. If it were, then the same result should be expected by varying the spacetime dimensions rather than mass. We show that this is intrinsically due to mass rather than the violation of the strong Huygens principle in Figure 3 for the weak coupling regime. Here we can see clearer in the rightmost figures a-ii)-c-ii) that mass generically improves entan-

glement generation, in that it always produces at least as much entanglement as the massless case, as is the case in  $(4+1)$ D and  $(5+1)$ D. In  $(2+1)$ D, the separation between massless and massive case is huge: we see that the massless field can only generate half as large negativity as the massive case. What is true in general, however, is that massive fields attain maximum entanglement *much slower* than the massless field. We note in passing that the entanglement cone is steeper as the spacetime dimension is increased — this is itself not surprising, as this can be explained by the fact that the Wightman two-point functions has stronger decay (in both space and time directions) in higher dimensions. It implies that generating entanglement for a given separation is harder in higher spacetime dimensions.

Now that we singled out mass as the factor that con-

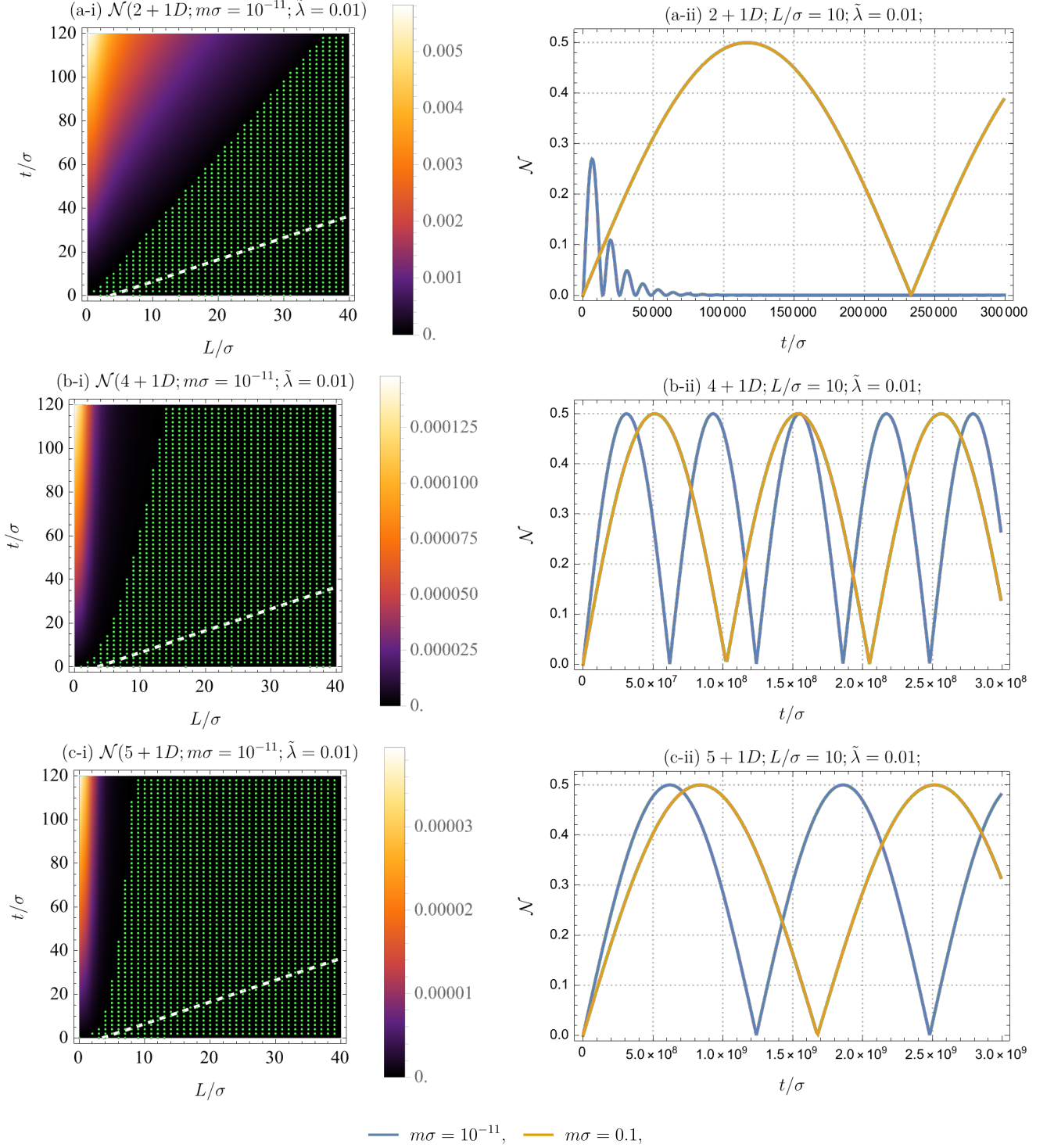


FIG. 3. Density plots [(a-i), (b-i), and (c-i)] of negativity  $\mathcal{N}$  between two inertial detectors weakly coupled ( $\tilde{\lambda} = 0.01$ ) to the nearly massless field in various spacetime dimensions. Here,  $\tilde{\lambda} \equiv \lambda\sigma^{-(n-3)/2}$  for  $(n+1)$ -dimensional Minkowski spacetime. On the right panel [(a-ii), (b-ii), and (c-ii)], the time dependence of  $\mathcal{N}$  at  $L/\sigma = 10$  with  $m\sigma = 10^{-11}$  (blue plots) and  $m\sigma = 0.1$  (orange plots) are depicted.

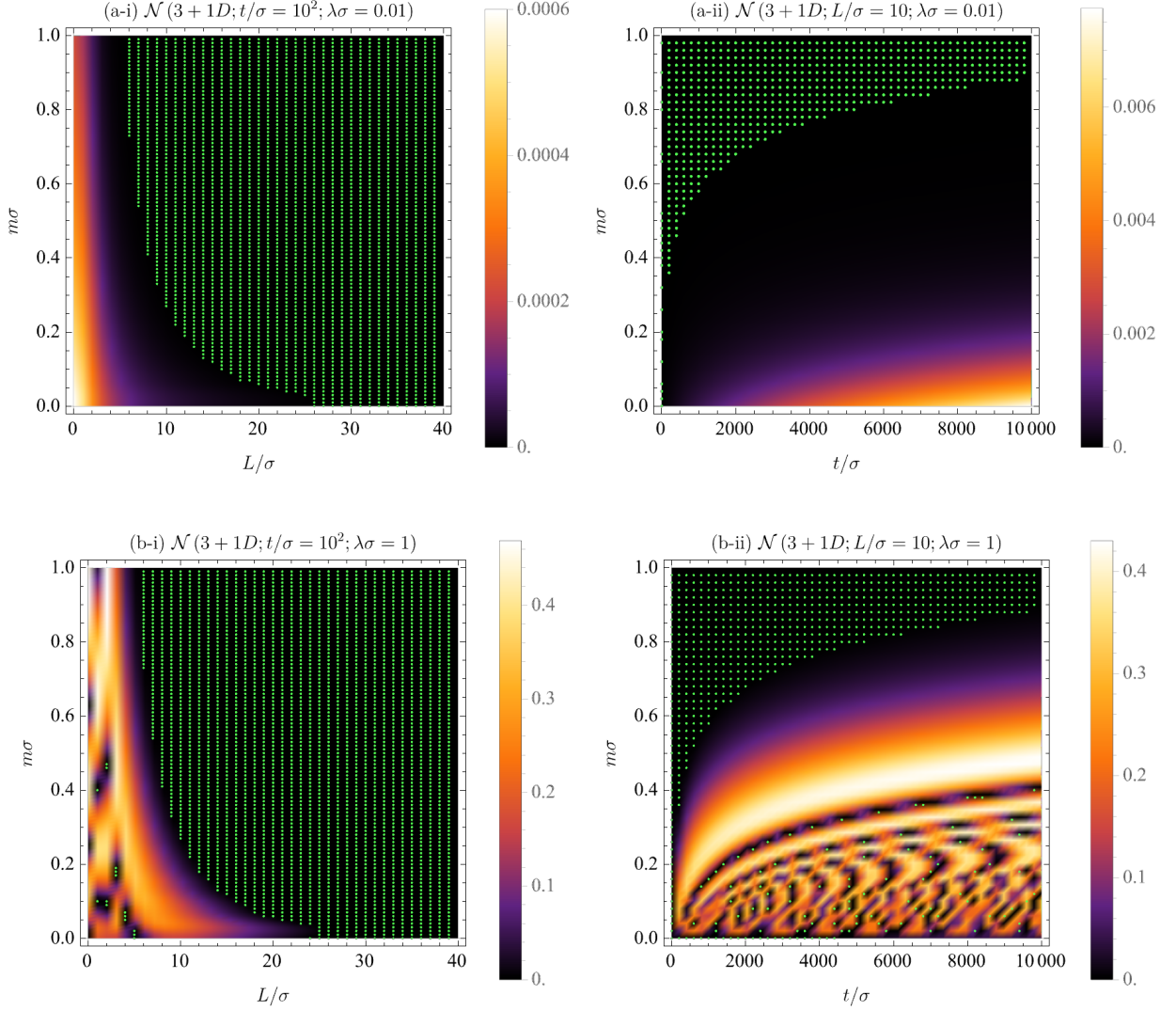


FIG. 4. Density plots of negativity  $\mathcal{N}$  between two inertial detectors in (3+1)-dimensional Minkowski spacetime, showing how mass  $m$  of the field contributes to  $\mathcal{N}$ . (a) and (b) correspond to the weak coupling  $\tilde{\lambda} = 0.01$  and strong coupling  $\tilde{\lambda} = 1$  cases. (a-i) and (b-i) depict the dependence on  $m\sigma$  and  $L/\sigma$  at a fixed time  $t/\sigma = 10^2$ , whereas (a-ii) and (b-ii) show the dependence on  $m\sigma$  and  $t/\sigma$  at a fixed distance  $L/\sigma = 10$ .

tributes to the enhancement of entanglement between the two detectors, it is useful to see how entanglement pattern changes with mass as we fix either spatial separation or duration of interaction, as shown in Figure 4. Here we see that the properties of spatial and temporal correlations of the field are indeed asymmetric and influences the negativity differently.<sup>10</sup> Notice that in Figures (a-i) and (b-i), we understand in what sense massless fields are more helpful: the larger the mass, the faster the negativity vanishes as a function of  $L$ , hence massless fields has “larger reach” in spatial separation as negativity vanishes at larger separation. Figures (a-ii) and (b-ii) complement our observations earlier: mass generically improves the maximum amount of entanglement generated on the detectors, in this case for the strong coupling regime relative to the weak-coupling one.

We summarize the main results as follows:

- (i) Non-perturbatively, gapless models can indeed generate entanglement between the two detectors, but they generically do so *very deep into the light cone*. This is in contrast to the standard perturbative result where entanglement is generated starting at the light cone (in other words, light cone and entanglement cone coincides) [41]. This is a stronger result than the no-go theorem in [22], which only proves that entanglement cannot be generated at spacelike-separation, since we showed that it is not enough that their interactions are in causal contact.
- (ii) Mass can improve entanglement generated relative to massless case in terms of the amount of negativity, sometimes approaching maximal entanglement  $\mathcal{N} \approx 0.5$  when massless field cannot. This is independent of the violation of the strong Huygens property. However, in general, massive fields only achieve maximum negativity at much longer interaction time, consistent with the fact that the entanglement cone is steeper with increasing mass.
- (iii) There is clear asymmetry between decay of correlations in spatial and temporal directions, which manifests as the difference in how negativity of the two detectors decay as a function of time and spatial separation for different mass parameters.

#### IV. ENTANGLEMENT DYNAMICS BETWEEN THREE DETECTORS

In this section, we study the entanglement dynamics between three gapless RSB-type UDW detectors inter-

acting with a scalar field initialized in the uncorrelated ground state of the non-interacting theory ( $\lambda_j = 0$ ) given by

$$|\psi(0)\rangle = |g_A\rangle |g_B\rangle |g_C\rangle |0\rangle. \quad (25)$$

For simplicity, the three detectors are assumed to be static and placed symmetrically at the vertices of an equilateral triangle, each separated by a distance  $L$  from one another [42]. This simplification is also helpful when trying to isolate the physics associated with the detector-field dynamics from the non-uniformity introduced by the asymmetric placement of the detectors.

Due to the relatively painful amount of computations, tripartite dynamics in the standard UDW model is already sparse. The relevant known results so far are:

- (i) Perturbatively, it was shown in Minkowski spacetime that three UDW detectors can extract tripartite entanglement at spacelike separation in various spatial configurations, not only the equilateral one [42]. This is also demonstrated for (2+1)D BTZ black hole spacetime [43]. The authors used  $\pi$ -tangle [86] that serves as a lower bound for the amount of genuine tripartite entanglement in mixed states of three qubits. It is noteworthy that  $\pi$ -tangle is not an entanglement measure on its own. There were some earlier studies that show W-type entanglement in entanglement harvesting-type setups (i.e., for spacelike-separated detectors) [87].
- (ii) Non-perturbatively, it was shown for Minkowski [28] that three UDW detectors can get entangled for *delta-coupled* detector model, also using  $\pi$ -tangle as a ‘witness’ of genuine tripartite entanglement. They show that there exist parameter regimes for which the tripartite entanglement is GHZ-type.

As before, we do not aim for an exhaustive list. From these, we believe that the long-time regime involving the gapless model has not been fully understood prior to this work. Let us remark that the regularity requirements for the three-detector RSB model follows directly from the general case in Section IID and Appendix A.

It is well-known that constructing entanglement measures for multipartite entanglement is highly non-trivial. Even for the case of three qubits, it is known that it is not possible to have a single entanglement measure that unambiguously tells whether one state is more entangled than another [88]. This is related to the fact that for multipartite entanglement one can have inequivalent but *genuine multipartite entanglement* (GME): the simplest examples being the GHZ and W states, which are in some sense “maximally entangled” (see, e.g., [89]). For our purposes, this issue is complicated by the fact that if we consider the RSB model with three detectors, then the reduced density matrix of the detector is mixed: for mixed states, constructing faithful entanglement measure

<sup>10</sup> Note that the asymmetry in the way correlations decay in the spatial and temporal directions is not unique to relativistic scalar fields: it is a well-known phenomenon in quantum many-body and condensed matter physics, which underlies why quantum many-body dynamics is a hard problem even for systems with exponentially decaying spatial correlations.

is generically difficult, and none of the convex-roof extensions (if at all) are easy to compute for mixed states.

In order to analyse the tripartite entanglement, we follow [28, 42, 43] and consider the  $\pi$ -tangle, defined as

$$\pi := \frac{\pi_A + \pi_B + \pi_C}{3}, \quad (26a)$$

$$\pi_A := \mathcal{N}_{A(BC)}^2 - \mathcal{N}_{A(B)}^2 - \mathcal{N}_{A(C)}^2, \quad (26b)$$

$$\pi_B := \mathcal{N}_{B(CA)}^2 - \mathcal{N}_{B(C)}^2 - \mathcal{N}_{B(A)}^2, \quad (26c)$$

$$\pi_C := \mathcal{N}_{C(AB)}^2 - \mathcal{N}_{C(A)}^2 - \mathcal{N}_{C(B)}^2. \quad (26d)$$

Here,

$$\mathcal{N}_{A(BC)} := \frac{\|\rho_{ABC}^{\text{TA}}\|_1 - 1}{2}, \quad (27a)$$

$$\mathcal{N}_{A(B)} := \frac{\|\rho_{AB}^{\text{TA}}\|_1 - 1}{2}, \quad (27b)$$

$$\mathcal{N}_{A(C)} := \frac{\|\rho_{AC}^{\text{TA}}\|_1 - 1}{2}, \quad (27c)$$

are the negativities of the three-detector system. The  $\pi$ -tangle quantifies the tripartite entanglement if the joint state of the detectors  $\rho_{ABC}$  is pure due to the Coffman-Kundu-Wootters inequality for negativity,  $\pi_i \geq 0$ ,  $\forall i \in \{A, B, C\}$  [86, 90]. Unfortunately, this property fails when  $\rho_{ABC}$  is mixed, and the  $\pi$ -tangle serves only as a lower bound for the tripartite entanglement. This suggests that the  $\pi$ -tangle for mixed states could be zero or negative, even if there exists tripartite entanglement among the detectors. Nevertheless, tripartite entanglement is guaranteed at least when the  $\pi$ -tangle is positive. For this reason, in what follows we take  $\max\{\pi, 0\}$  and examine the parameter space with positive  $\pi$ -tangle.

This time, it will be useful to first summarize our results for the tripartite entanglement dynamics involving the gapless RSB model:

- (i) There exists a regime in the parameter space for which the three detectors have *genuine tripartite entanglement* of the ‘‘GHZ type’’, in the sense that for any bipartition has zero entanglement. However, this regime is generically very narrow and has very small  $\pi$ -tangle, thus it is difficult to certify that the tripartite entanglement is significant.
- (ii) A large portion of the parameter space allows for tripartite entanglement such that any bipartition has nonzero entanglement. Similar to the bipartite case, mass of the field tends to amplify the  $\pi$ -tangle, but there is no natural way to discern the nature of the tripartite entanglement.

We will provide arguments for why this is the case and put the existing known results in perspectives.

Our argument is based on a numerical analysis in Figure 5 for both weak and strong coupling as well as massless and massive fields. The white dashed line represents the light cone. What we show here is that on the one

hand, the black region below the red line in Figure 5 corresponds to the case for which the three detectors have *genuine tripartite entanglement* of the ‘‘GHZ type’’, in the sense that for any bipartition has zero entanglement. However, this region is generically very narrow, thus one has to fine-tune the arrangement of the detectors to obtain this. Furthermore, since the  $\pi$ -tangle is very small, it is difficult to certify that this genuine tripartite entanglement is actually significant. On the other hand, the area bounded by the green dots above the red line shows the regime that allows for tripartite entanglement with nonzero bipartite entanglement. We also observe that mass of the field tends to amplify the  $\pi$ -tangle, however there is no natural way to obtain precise information about the nature of the tripartite entanglement. Indeed, we checked that none of the usual tripartite entanglement witness for mixed states works [91], as we verified them numerically and all of them are inconclusive (i.e., they say nothing about the tripartite entanglement content). These results seem to suggest that there are significant limitations in using gapless UDW or RSB-type models to learn about both intrinsic multipartite entanglement and multipartite entanglement generation in QFT.

A natural question to ask is how this result is compatible with the observations in [28], which essentially claim that there is genuine tripartite entanglement of GHZ type in Minkowski spacetime and BTZ spacetime for the vacuum state of a massless scalar field with delta-coupled model. Strictly speaking, while there are some similarities between delta-coupled model and the gapless model [27], the results in [28] is not ideal as they showed genuine tripartite entanglement only for very small detector separation, effectively with significant overlap of their Gaussian smearing functions. In this regime, one can question the validity of the standard UDW model. This is because very closely-spaced atoms may experience interatomic interactions that the UDW model we considered here does not capture. In this sense, our results are more reliable as they do not rely on significant overlap of the spatial smearing and still displays genuine tripartite entanglement of GHZ type.

## V. DISCUSSION AND OUTLOOK

In this work we have studied non-perturbatively the entanglement generation between two emitters in an exactly solvable relativistic variant of the spin-boson model, equivalent to the time-independent formulation of the (gapless) Unruh-DeWitt model. This formulation allows for rigorous basis of the regularity of the model in the UV and in the IR and allows slightly cleaner analysis of the causal behaviour of the interactions.

We showed that (i) (highly) entangled states of the two emitters (detectors) require interactions *very deep into the light cone*, strengthening the no-go result of [22] that says there can be no entanglement for spacelike-separated interactions; (ii) the mass of the field gener-

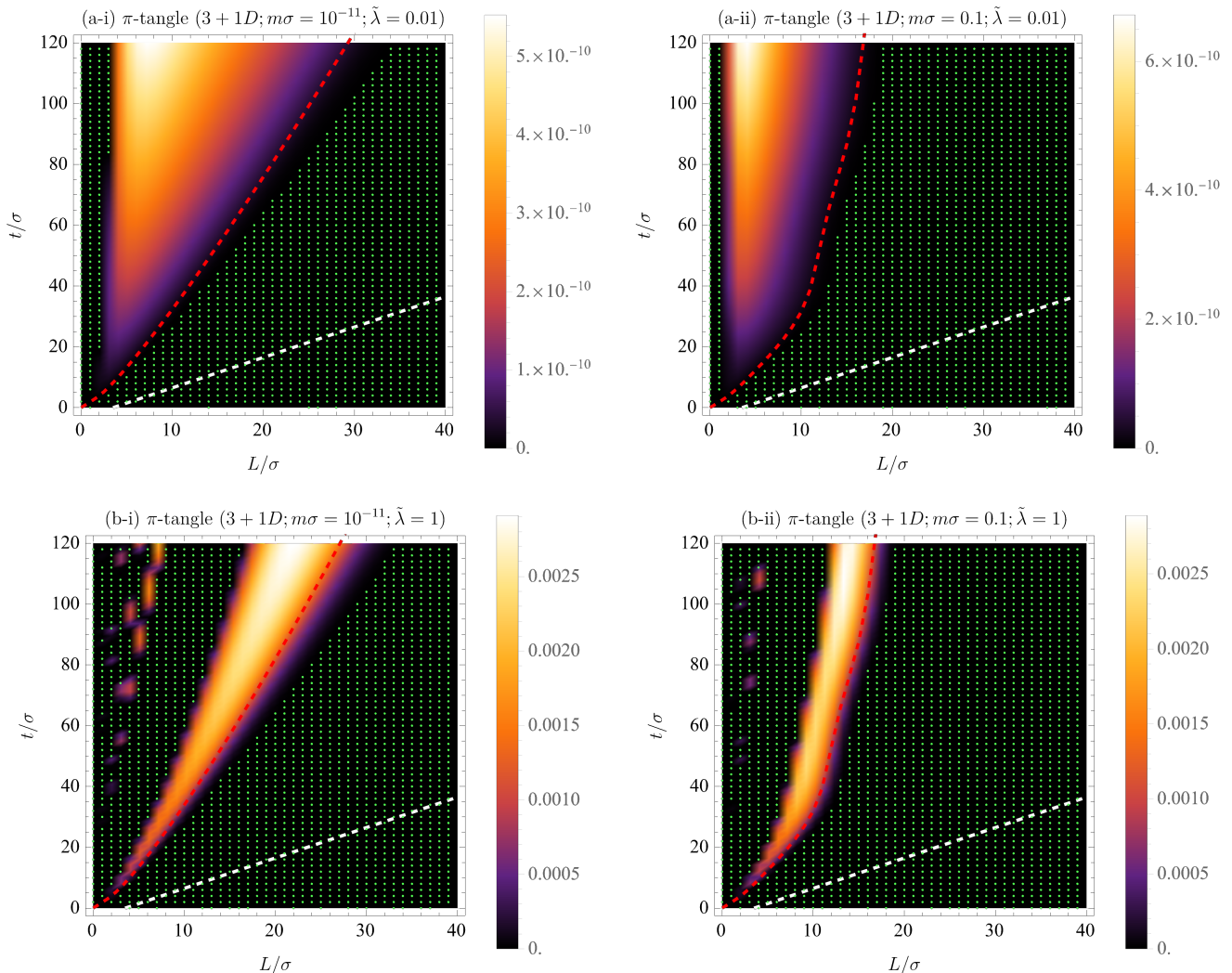


FIG. 5. Density plots of the positive  $\pi$ -tangle among three inertial detectors in the equilateral triangular configuration in  $(3+1)$ -dimensional Minkowski spacetime when the detectors are (a) weakly coupled, and (b) strongly coupled to the field. (a-i) and (b-i) show the nearly massless ( $m\sigma = 10^{-11}$ ) scenario, whereas (a-ii) and (b-ii) correspond to the massive case with  $m\sigma = 0.1$ . The green dots depict the region where the  $\pi$ -tangle vanishes. The white dashed line represents the light cone from the edge of the detector as before, while the red dashed curve corresponds to the boundary of the bipartite entanglement cone depicted in Figs. 1 and 2.

ically improves the maximum amount of entanglement generated on the detectors at the expense of longer interaction times and furthermore, we argued that this is not fundamentally due to the strong Huygens principle; (iii) unlike the bipartite case where it is possible to generate close to maximally entangled states via the spin-boson interactions, the generation of genuine tripartite entanglement for sufficiently separated detectors is non-perturbatively hard even at sufficiently long times, refining the delta-coupling result in [28]. Result (iii), in particular, suggests that probing the multipartite entanglement of a relativistic quantum field non-perturbatively requires either different probe-based techniques or variants of the UDW model.

In a way, our results suggest that despite the non-perturbative and simple nature of the model, the gapless variant of the UDW model is not good enough once we are interested in obtaining more precise information about multipartite entanglement, whether to study the intrinsic multipartite entanglement in the field or the ability for relativistic quantum fields to mediate entanglement generation. From the quantum-optical standpoint, it means that this model is not very useful for generating highly-entangled multipartite entangled states *even if we allow causal contact*, and since this model is unable to extract entanglement from the vacuum state at spacelike separation, we can think of the gapless model as being suitable, for instance, in studying classical communica-

tion settings (see, e.g., [26]). That said, our work closes the (remaining) gap for the two-detector scenario: we showed that causal contact enables entanglement generation in a maximal sense, but this requires the interaction time to be much larger than the spatial separation of the detectors, in contrast to the known perturbative results [41].

Three natural questions arise from our work. First, is it possible to consider a variant of the setup or the model in such a way that we can probe non-perturbatively multipartite entanglement of the vacuum state of the field in a useful way? Presumably, there are operator-algebraic approach to studying multipartite entanglement [92] of the QFT directly, and this should ideally be complementary. Second, can multiple delta-coupled detectors be used more effectively to study entanglement in QFT? The first use case was in [22], and recently multi-delta coupling has been used in single-detector settings [24, 93]. These quickly become unwieldy for large number of couplings and detectors, but in principle computable. Last but not least, one way to resolve the ambiguity regarding the nature and “strength” of the tripartite entanglement is by operational means, i.e., by identifying protocols (e.g., teleportation in or steering in the bipartite case) that requires certain kinds and amount of tripartite entanglement to succeed and see if the tripartite state produced via the RSB interaction works for these protocols. We leave these questions for the future.

### ACKNOWLEDGMENT

E.T. acknowledges financial support from the Alexander von Humboldt Foundation. K.G.Y. is partially supported by Grant-in-Aid for Research Activity Start-up (Grant No. JP24K22862) and by Grant-in-Aid for JSPS Fellows (Grant No. JP25KJ0048).

### Appendix A: Regularity for N-partite RSB model

*Proof of Proposition 1.* For the sake of generality, we consider  $N$  detectors A, B, C, ..., coupled to the quantum scalar field  $\hat{\phi}$ . Let  $|\pm_j\rangle$  be the eigenvectors of  $\hat{\sigma}_x^{(j)}$ ,  $j \in \{A, B, C, \dots\}$  with the eigenvalues  $\pm 1$ , respectively. Using the expressions  $\hat{\sigma}_x^{(j)} = |+_j\rangle\langle+_j| - |-_j\rangle\langle-_j|$  and  $\mathbb{1}_j = |+_j\rangle\langle+_j| + |-_j\rangle\langle-_j|$ , the RSB Hamiltonian for gapless detectors can be expressed as follows:

$$\hat{H}_{0,\Delta,\lambda} = \sum_{\mathbf{s} \in \{\pm\}^N} |\mathbf{s}\rangle\langle\mathbf{s}| \otimes \hat{H}_{\mathbf{s}}, \quad (\text{A1})$$

where  $\mathbf{s} \in \{+, -\}^N$  is a vector composed of signs, and

$$\hat{H}_{\mathbf{s}} := \hat{H}_{\phi,0} + \mathbf{s} \cdot \mathbf{\Delta} \mathbb{1}_{\phi} + \hat{a}(\mathbf{s} \cdot \mathbf{F}^*) + \hat{a}^\dagger(\mathbf{s} \cdot \mathbf{F}), \quad (\text{A2})$$

where  $\mathbf{\Delta} \equiv [\Delta_A, \Delta_B, \dots]^\top$  is a vector of  $\Delta_j$ , and  $\mathbf{F}_{\mathbf{k}} \equiv [F_{\mathbf{k}}^{(A)}, F_{\mathbf{k}}^{(B)}, \dots]^\top$  is a vector of coupling functions. As an example, consider two detectors A and B (i.e., when  $N = 2$ ). In this case, we have  $|\mathbf{s}\rangle \in \{|+_A, +_B\rangle, |+_A, -_B\rangle, |-_A, +_B\rangle, |-_A, -_B\rangle\}$ , and so the gapless RSB Hamiltonian reads

$$\hat{H}_{0,\Delta,\lambda} = \sum_{p,q=\pm} |p_A\rangle\langle p_A| \otimes |q_B\rangle\langle q_B| \otimes \hat{H}_{p,q},$$

where

$$\begin{aligned} \hat{H}_{p,q} &= \hat{H}_{\phi,0} + (p\Delta_A + q\Delta_B) \mathbb{1}_{\phi} + \hat{a}(pF_{\mathbf{k}}^{(A)*} + qF_{\mathbf{k}}^{(B)*}) \\ &\quad + \hat{a}^\dagger(pF_{\mathbf{k}}^{(A)} + qF_{\mathbf{k}}^{(B)}). \end{aligned} \quad (\text{A3})$$

The operator  $\hat{H}_{\mathbf{s}}$  can be deformed into

$$\begin{aligned} \hat{H}_{\mathbf{s}} &= \int_{\mathbb{R}^n} d^n \mathbf{k} \left( \omega_{\mathbf{k}} \hat{a}_{\mathbf{k}}^\dagger \hat{a}_{\mathbf{k}} + \mathbf{s} \cdot \mathbf{F}_{\mathbf{k}}^* \hat{a}_{\mathbf{k}} + \mathbf{s} \cdot \mathbf{F}_{\mathbf{k}} \hat{a}_{\mathbf{k}}^\dagger + \frac{|\mathbf{s} \cdot \mathbf{F}_{\mathbf{k}}|^2}{\omega_{\mathbf{k}}} \mathbb{1}_{\phi} \right) \\ &\quad + \mathbf{s} \cdot \mathbf{\Delta} \mathbb{1}_{\phi} - \int_{\mathbb{R}^n} d^n \mathbf{k} \frac{|\mathbf{s} \cdot \mathbf{F}_{\mathbf{k}}|^2}{\omega_{\mathbf{k}}} \mathbb{1}_{\phi} \\ &= \hat{H}_{\phi,0,\mathbf{s}} + [\mathbf{s} \cdot \mathbf{\Delta} - R_1(\mathbf{s} \cdot \mathbf{F}_{\mathbf{k}}, n)] \mathbb{1}_{\phi}, \end{aligned} \quad (\text{A4})$$

where we have defined

$$\begin{aligned} \hat{H}_{\phi,0,\mathbf{s}} &:= \int_{\mathbb{R}^n} d^n \mathbf{k} \omega_{\mathbf{k}} \hat{c}_{\mathbf{k},\mathbf{s}}^\dagger \hat{c}_{\mathbf{k},\mathbf{s}}, \quad (\text{A5}) \\ \hat{c}_{\mathbf{k},\mathbf{s}} &:= \hat{a}_{\mathbf{k}} + \frac{\mathbf{s} \cdot \mathbf{F}_{\mathbf{k}}}{\omega_{\mathbf{k}}} \mathbb{1}_{\phi} \\ &= \hat{D}^\dagger(\mathbf{s} \cdot \mathbf{F}_{\mathbf{k}}/\omega_{\mathbf{k}}) \hat{a}_{\mathbf{k}} \hat{D}(\mathbf{s} \cdot \mathbf{F}_{\mathbf{k}}/\omega_{\mathbf{k}}). \end{aligned} \quad (\text{A6})$$

Here,  $\hat{D}(\alpha_{\mathbf{k}})$  is the displacement operator. One can straightforwardly show that the field's free Hamiltonian  $\hat{H}_{\phi,0}$  is unitarily equivalent to  $\hat{H}_{\phi,0,\mathbf{s}}$  via a transformation:

$$\hat{H}_{\phi,0,\mathbf{s}} = \hat{D}^\dagger(\alpha_{\mathbf{s}}) \hat{H}_{\phi,0} \hat{D}(\alpha_{\mathbf{s}}), \quad \alpha_{\mathbf{s}} := \int_{\mathbb{R}^n} d^n \mathbf{k} \frac{\mathbf{s} \cdot \mathbf{F}_{\mathbf{k}}}{\omega_{\mathbf{k}}}. \quad (\text{A7})$$

This suggests that the ground state of  $\hat{H}_{\phi,0,\mathbf{s}}$  is given by the coherent state  $|\alpha_{\mathbf{s}}\rangle \equiv \hat{D}^\dagger(\alpha_{\mathbf{s}}) |0\rangle$ , where  $|0\rangle$  is the Fock vacuum of the free Hamiltonian  $\hat{H}_{\phi,0}$ . Therefore, defining  $|\psi_0^{(\mathbf{s})}\rangle := |\mathbf{s}\rangle \otimes |\alpha_{\mathbf{s}}\rangle$ ,  $\mathbf{s} \in \{\pm\}^N$ , we obtain

$$\langle \hat{H}_{0,\Delta,\lambda} \rangle = \mathbf{s} \cdot \mathbf{\Delta} - R_1(\mathbf{s} \cdot \mathbf{F}_{\mathbf{k}}, n). \quad (\text{A8})$$

□

## Appendix B: Joint density matrix for gapless detectors

### 1. General expression of the reduced density matrix for an $N$ -partite system

In this section, we derive the joint density matrix for  $N$  gapless detectors in  $(n+1)$ -dimensional spacetime. Suppose the initial state for the total system is

$$\begin{aligned} |\psi(0)\rangle &= \underbrace{|g_A\rangle |g_B\rangle \cdots}_{N} \otimes |0\rangle \\ &= \sum_{\mathbf{s} \in \{\pm\}^N} \frac{1}{2^{N/2}} |\mathbf{s}\rangle \otimes |0\rangle, \end{aligned} \quad (\text{B1})$$

where  $|g_j\rangle$  is the ground state of  $\hat{\sigma}_z^{(j)}$ , and  $|0\rangle$  is the Fock vacuum of the field's free Hamiltonian  $\hat{H}_{\phi,0}$ . The second equality is derived by using  $|g_j\rangle = (|+_j\rangle + |-_j\rangle)/\sqrt{2}$ .

The total system of  $N$  gapless qubits and the field evolves under a unitary operator generated by the gapless RSB Hamiltonian:  $\hat{U}(t) = e^{-it\hat{H}_{0,\Delta,\lambda}}$ . As we have seen in Eq. (A1), the gapless RSB Hamiltonian takes the diagonalized form in the basis  $\{|\mathbf{s}\rangle \mid \mathbf{s} \in \{\pm\}^N\}$ . Therefore, the unitary operator  $\hat{U}(t)$  can also be diagonalized in this basis, which can be expressed as

$$\hat{U}(t) = \sum_{\mathbf{s} \in \{\pm\}^N} |\mathbf{s}\rangle \langle \mathbf{s}| \otimes e^{-it\hat{H}_s}, \quad (\text{B2})$$

and the total state  $|\psi(t)\rangle$  at time  $t$  can be compactly written as

$$\begin{aligned} |\psi(t)\rangle &= \hat{U}(t) |\psi(0)\rangle \\ &= \frac{1}{2^{N/2}} \sum_{\mathbf{s} \in \{\pm\}^N} |\mathbf{s}\rangle \otimes e^{-it\hat{H}_s} |0\rangle. \end{aligned} \quad (\text{B3})$$

The reduced density matrix for the  $N$  gapless qubits thus reads

$$\begin{aligned} \rho(t) &= \text{Tr}_\phi[|\psi(t)\rangle \langle \psi(t)|] \\ &= \frac{1}{2^N} \sum_{\mathbf{s}, \mathbf{r} \in \{\pm\}^N} \langle 0 | e^{it\hat{H}_s} e^{-it\hat{H}_r} |0\rangle |\mathbf{r}\rangle \langle \mathbf{s}|. \end{aligned} \quad (\text{B4})$$

In the case of the bipartite qubit system ( $N=2$ ), the RSB Hamiltonian in the basis  $\{|++\rangle, |+-\rangle, |-+\rangle, |--\rangle\}$  is expressed as

$$\hat{H}_{0,\Delta,\lambda} = \begin{bmatrix} \hat{H}_{++} & 0 & 0 & 0 \\ 0 & \hat{H}_{+-} & 0 & 0 \\ 0 & 0 & \hat{H}_{-+} & 0 \\ 0 & 0 & 0 & \hat{H}_{--} \end{bmatrix},$$

where  $H_{p,q}$ ,  $p, q \in \{\pm\}$  is given by (A3), and the unitary

operator generated by this Hamiltonian is thus

$$\hat{U}(t) = \begin{bmatrix} e^{-it\hat{H}_{++}} & 0 & 0 & 0 \\ 0 & e^{-it\hat{H}_{+-}} & 0 & 0 \\ 0 & 0 & e^{-it\hat{H}_{-+}} & 0 \\ 0 & 0 & 0 & e^{-it\hat{H}_{--}} \end{bmatrix}.$$

To obtain the reduced density matrix  $\rho(t)$ , we need to evaluate the vacuum expectation value  $\langle 0 | e^{it\hat{H}_s} e^{-it\hat{H}_r} |0\rangle$ . To do this, we utilize the following:

$$\begin{aligned} e^{it\hat{H}_s} e^{-it\hat{H}_r} &= e^{it(\mathbf{s}-\mathbf{r})\cdot\Delta} e^{i[\theta_s(t)-\theta_r(t)]} e^{i\text{Im}(\eta_{\mathbf{k}}(t)\mathbf{s}\cdot\mathbf{F}_{\mathbf{k}})\mathcal{H}} e^{i\omega_{\mathbf{k}}t/2} \\ &\quad \times W((\mathbf{s}-\mathbf{r})\cdot\mathbf{F}_{\mathbf{k}}\eta_{\mathbf{k}}(t)e^{i\omega_{\mathbf{k}}t}), \end{aligned} \quad (\text{B5})$$

where

$$\theta_{\mathbf{s}}(t) := \int_{\mathbb{R}^n} d^n \mathbf{k} \frac{|\mathbf{s}\cdot\mathbf{F}_{\mathbf{k}}|^2}{\omega_{\mathbf{k}}^2} (\sin(\omega_{\mathbf{k}}t) - \omega_{\mathbf{k}}t), \quad (\text{B6})$$

$$(f_{\mathbf{k}}, g_{\mathbf{k}})\mathcal{H} := \int_{\mathbb{R}^n} d^n \mathbf{k} f_{\mathbf{k}}^* g_{\mathbf{k}}, \quad (\text{B7})$$

$$\eta_{\mathbf{k}}(t) := \frac{2e^{-i\omega_{\mathbf{k}}t/2}}{\omega_{\mathbf{k}}} \sin(\omega_{\mathbf{k}}t/2). \quad (\text{B8})$$

This can be derived straightforwardly from Lemma 1 in [29], which employs a Lie algebraic technique (see Sec. 7.4 in [94]) to decompose  $e^{it\hat{H}_s}$  into products of exponentials:

$$e^{it\hat{H}_s} = e^{it\mathbf{s}\cdot\Delta} e^{i\theta_s(t)} e^{it\hat{H}_{\phi,0}} e^{i\hat{\phi}(\eta_{\mathbf{k}}(t)\mathbf{s}\cdot\mathbf{F}_{\mathbf{k}})}. \quad (\text{B9})$$

Realizing that  $e^{i\hat{\phi}(\eta_{\mathbf{k}}(t)\mathbf{s}\cdot\mathbf{F}_{\mathbf{k}})}$  is an element of the Weyl algebra  $W(\eta_{\mathbf{k}}(t)\mathbf{s}\cdot\mathbf{F}_{\mathbf{k}}) \equiv e^{i\hat{\phi}(\eta_{\mathbf{k}}(t)\mathbf{s}\cdot\mathbf{F}_{\mathbf{k}})}$ , the Weyl relation [29]  $W(f_{\mathbf{k}})W(g_{\mathbf{k}}) = e^{-i\text{Im}(f_{\mathbf{k}}, g_{\mathbf{k}})\mathcal{H}} W(f_{\mathbf{k}} + g_{\mathbf{k}})$  leads to Eq. (B5). From Eq. (B5), we have the reduced density matrix for the  $N$  gapless qubits:

$$\begin{aligned} \rho(t) &= \frac{1}{2^N} \sum_{\mathbf{s}, \mathbf{r} \in \{\pm\}^N} |\mathbf{r}\rangle \langle \mathbf{s}| e^{it(\mathbf{s}-\mathbf{r})\cdot\Delta} e^{i[\theta_s(t)-\theta_r(t)]} \\ &\quad \times e^{i\text{Im}(\eta_{\mathbf{k}}(t)\mathbf{s}\cdot\mathbf{F}_{\mathbf{k}}, \eta_{\mathbf{k}}(t)\mathbf{r}\cdot\mathbf{F}_{\mathbf{k}})\mathcal{H}} \omega_0(W((\mathbf{s}-\mathbf{r})\cdot\mathbf{F}_{\mathbf{k}}\eta_{\mathbf{k}}^*(t))), \end{aligned} \quad (\text{B10})$$

where  $\omega_0(W(f_{\mathbf{k}})) \equiv \langle 0 | e^{i\hat{\phi}(f_{\mathbf{k}})} |0\rangle$  with  $\omega_0 : \mathcal{W}(\mathcal{M}) \rightarrow \mathbb{C}$  being the state corresponding to the Fock vacuum  $|0\rangle$ . Practically, this can be evaluated in the following way:

$$\omega_0(W(f_{\mathbf{k}})) = \exp\left(-\frac{1}{2} \int_{\mathbb{R}^n} d^n \mathbf{k} |f_{\mathbf{k}}|^2\right). \quad (\text{B11})$$

Needless to say, a concrete expression of  $\rho(t)$  requires an explicit form of  $F_{\mathbf{k}}^{(j)}$ . In the following subsections, we obtain the expression of each element in  $\rho(t)$  for the bipartite and tripartite cases when the background spacetime geometry is flat.

## 2. Two gapless qubits in Minkowski spacetime

As a concrete example, we restrict ourselves to  $(n+1)$ -dimensional Minkowski spacetime and consider two static detectors with zero relative velocity. For the sake of convenience, we choose the following Gaussian spatial smearing profile:

$$F^{(j)}(\mathbf{x}) = \frac{1}{(\sqrt{\pi}\sigma)^n} e^{-\frac{(\mathbf{x}-\mathbf{x}_{j0})^2}{\sigma^2}}, \quad j \in \{A, B\}. \quad (\text{B12})$$

Here,  $\sigma > 0$  is the characteristic Gaussian width and  $\mathbf{x}_{j0}$  is the center of the smearing function. This smearing function is Fourier transformed into

$$\begin{aligned} F_{\mathbf{k}}^{(j)} &:= \int_{\Sigma_0} d^n x \sqrt{h_0} \lambda_j F^{(j)}(\mathbf{x}) u_{\mathbf{k}}^*(0, \mathbf{x}) \\ &= \int_{\mathbb{R}^n} \frac{d^n x}{\sqrt{2\omega_{\mathbf{k}}(2\pi)^n}} \lambda_j F^{(j)}(\mathbf{x}) e^{i\mathbf{k}\cdot\mathbf{x}} \\ &= \frac{\lambda_j e^{-|\mathbf{k}|^2 \sigma^2/4} e^{i\mathbf{k}\cdot\mathbf{x}_{j0}}}{\sqrt{2\omega_{\mathbf{k}}(2\pi)^n}}. \end{aligned} \quad (\text{B13})$$

Define the distance  $L$  between the detectors as  $L :=$

$|\mathbf{x}_{A,0} - \mathbf{x}_{B,0}|$ . From Eq. (B10), the reduced density matrix  $\rho_{AB}(t)$  in the basis  $\{|++\rangle, |+-\rangle, |-+\rangle, |--\rangle\}$  reads

$$\rho_{AB}(t) = \frac{1}{4} \begin{bmatrix} 1 & \rho_{12} & \rho_{13} & \rho_{14} \\ \rho_{12}^* & 1 & \rho_{23} & \rho_{24} \\ \rho_{13}^* & \rho_{23}^* & 1 & \rho_{34} \\ \rho_{14}^* & \rho_{24}^* & \rho_{34}^* & 1 \end{bmatrix}, \quad (\text{B14})$$

with

$$\rho_{12} = e^{-2it\Delta_B} e^{-i\vartheta_{AB}} \omega_0(W(F_{\mathbf{k}}^{(B)} \eta_{\mathbf{k}}^*(t))), \quad (\text{B15a})$$

$$\rho_{13} = e^{-2it\Delta_A} e^{-i\vartheta_{AB}} \omega_0(W(F_{\mathbf{k}}^{(A)} \eta_{\mathbf{k}}^*(t))), \quad (\text{B15b})$$

$$\begin{aligned} \rho_{14} &= e^{-2it(\Delta_A + \Delta_B)} e^{-\Xi_{AB}} \\ &\quad \times \omega_0(W(F_{\mathbf{k}}^{(A)} \eta_{\mathbf{k}}^*(t))) \omega_0(W(F_{\mathbf{k}}^{(B)} \eta_{\mathbf{k}}^*(t))), \end{aligned} \quad (\text{B15c})$$

$$\begin{aligned} \rho_{23} &= e^{-2it(\Delta_A - \Delta_B)} e^{\Xi_{AB}} \\ &\quad \times \omega_0(W(F_{\mathbf{k}}^{(A)} \eta_{\mathbf{k}}^*(t))) \omega_0(W(F_{\mathbf{k}}^{(B)} \eta_{\mathbf{k}}^*(t))), \end{aligned} \quad (\text{B15d})$$

$$\rho_{24} = e^{-2it\Delta_A} e^{i\vartheta_{AB}} \omega_0(W(F_{\mathbf{k}}^{(A)} \eta_{\mathbf{k}}^*(t))), \quad (\text{B15e})$$

$$\rho_{34} = e^{-2it\Delta_B} e^{i\vartheta_{AB}} \omega_0(W(F_{\mathbf{k}}^{(B)} \eta_{\mathbf{k}}^*(t))), \quad (\text{B15f})$$

where

$$\omega_0(W(F_{\mathbf{k}}^{(j)} \eta_{\mathbf{k}}^*(t))) = \exp\left(-\frac{8\lambda_j^2}{(2\pi)^n} \frac{\sqrt{\pi^n}}{\Gamma(n/2)} \int_0^\infty d|\mathbf{k}| \frac{|\mathbf{k}|^{n-1} \sin^2(\omega_{\mathbf{k}} t/2)}{\omega_{\mathbf{k}}^3} e^{-|\mathbf{k}|^2 \sigma^2/2}\right), \quad (\text{B16a})$$

$$\vartheta_{AB} = \frac{4\lambda_A \lambda_B}{(2\pi)^n} \sqrt{\pi^n} \int_0^\infty d|\mathbf{k}| \frac{|\mathbf{k}|^{n-1} e^{-|\mathbf{k}|^2 \sigma^2/2}}{\omega_{\mathbf{k}}^3} (\sin(\omega_{\mathbf{k}} t) - \omega_{\mathbf{k}} t) {}_0\mathcal{F}_1\left(\frac{n}{2}; -\frac{|\mathbf{k}|^2 L^2}{4}\right), \quad (\text{B16b})$$

$$\Xi_{AB} = \frac{16\lambda_A \lambda_B}{(2\pi)^n} \sqrt{\pi^n} \int_0^\infty d|\mathbf{k}| \frac{|\mathbf{k}|^{n-1} e^{-|\mathbf{k}|^2 \sigma^2/2}}{\omega_{\mathbf{k}}^3} \sin^2(\omega_{\mathbf{k}} t/2) {}_0\mathcal{F}_1\left(\frac{n}{2}; -\frac{|\mathbf{k}|^2 L^2}{4}\right). \quad (\text{B16c})$$

Here,  ${}_0\mathcal{F}_1$  is the regularized generalized hypergeometric function and  $\Gamma(z)$  is the Gamma function [95, 96]. We note that the phase term

$$e^{i\text{Im}(\eta_{\mathbf{k}}(t)\mathbf{s}\cdot\mathbf{F}_{\mathbf{k}}, \eta_{\mathbf{k}}(t)\mathbf{r}\cdot\mathbf{F}_{\mathbf{k}})}_{\mathcal{H}} = 1$$

as  $\text{Im}(\eta_{\mathbf{k}}(t)\mathbf{s}\cdot\mathbf{F}_{\mathbf{k}}, \eta_{\mathbf{k}}(t)\mathbf{r}\cdot\mathbf{F}_{\mathbf{k}})_{\mathcal{H}} = 0$  for a real smearing function  $F^{(j)}$ .<sup>11</sup>

## 3. Three gapless qubits in the equilateral triangular configuration

We now consider three static gapless detectors A, B, and C, in  $(n+1)$ -dimensional Minkowski spacetime. In

this tripartite case, we have the freedom to choose the spatial configuration of the detectors. The simplest one is the equilateral triangle configuration [28, 42, 43], namely, each detector is located at a corner of an equilateral triangle at each time  $t$ . Such a symmetrical configuration simplifies the calculation drastically, as the proper distance between any pair of the detectors is the same  $L$ .

From Eq. (B10) with  $N = 3$ , the reduced density matrix is an  $8 \times 8$  matrix,

$$\rho(t) = \frac{1}{8} \begin{bmatrix} 1 & \rho_{12} & \rho_{13} & \rho_{14} & \rho_{15} & \rho_{16} & \rho_{17} & \rho_{18} \\ \rho_{12}^* & 1 & \rho_{23} & \rho_{24} & \rho_{25} & \rho_{26} & \rho_{27} & \rho_{28} \\ \rho_{13}^* & \rho_{23}^* & 1 & \rho_{34} & \rho_{35} & \rho_{36} & \rho_{37} & \rho_{38} \\ \rho_{14}^* & \rho_{24}^* & \rho_{34}^* & 1 & \rho_{45} & \rho_{46} & \rho_{47} & \rho_{48} \\ \rho_{15}^* & \rho_{25}^* & \rho_{35}^* & \rho_{45}^* & 1 & \rho_{56} & \rho_{57} & \rho_{58} \\ \rho_{16}^* & \rho_{26}^* & \rho_{36}^* & \rho_{46}^* & \rho_{56}^* & 1 & \rho_{67} & \rho_{68} \\ \rho_{17}^* & \rho_{27}^* & \rho_{37}^* & \rho_{47}^* & \rho_{57}^* & \rho_{67}^* & 1 & \rho_{78} \\ \rho_{18}^* & \rho_{28}^* & \rho_{38}^* & \rho_{48}^* & \rho_{58}^* & \rho_{68}^* & \rho_{78}^* & 1 \end{bmatrix}, \quad (\text{B17})$$

in the basis  $\{|+++ \rangle, |++- \rangle, |+-+ \rangle, |-++ \rangle,$

<sup>11</sup> This is consistent with the fact that the causal propagator  $E(f, g)$  is zero when the supports of  $f$  and  $g$  are causally disconnected, as  $\text{Im}(f_{\mathbf{k}}, g_{\mathbf{k}})_{\mathcal{H}}$  is the “ $\mathbf{k}$ -space version” of  $E(f, g)$ . See [29].

$|+- -\rangle, |-+-\rangle, |--+\rangle, |---\rangle\}$ . Each element reads

$$\begin{aligned}
\rho_{12} &= e^{-2it\Delta_C} e^{i(\vartheta_{CA}+\vartheta_{BC})} \omega_0(W(F_{\mathbf{k}}^{(C)}\eta_{\mathbf{k}}^*(t))), \\
\rho_{13} &= e^{-2it\Delta_B} e^{i(\vartheta_{AB}+\vartheta_{BC})} \omega_0(W(F_{\mathbf{k}}^{(B)}\eta_{\mathbf{k}}^*(t))), \\
\rho_{14} &= e^{-2it\Delta_A} e^{i(\vartheta_{AB}+\vartheta_{CA})} \omega_0(W(F_{\mathbf{k}}^{(A)}\eta_{\mathbf{k}}^*(t))), \\
\rho_{15} &= e^{-2it(\Delta_B+\Delta_C)} e^{i(\vartheta_{AB}+\vartheta_{CA})} e^{-\Xi_{BC}} \\
&\quad \times \omega_0(W(F_{\mathbf{k}}^{(B)}\eta_{\mathbf{k}}^*(t)))\omega_0(W(F_{\mathbf{k}}^{(C)}\eta_{\mathbf{k}}^*(t))), \\
\rho_{16} &= e^{-2it(\Delta_A+\Delta_C)} e^{i(\vartheta_{AB}+\vartheta_{BC})} e^{-\Xi_{CA}} \\
&\quad \times \omega_0(W(F_{\mathbf{k}}^{(A)}\eta_{\mathbf{k}}^*(t)))\omega_0(W(F_{\mathbf{k}}^{(C)}\eta_{\mathbf{k}}^*(t))), \\
\rho_{17} &= e^{-2it(\Delta_A+\Delta_B)} e^{i(\vartheta_{CA}+\vartheta_{BC})} e^{-\Xi_{AB}} \\
&\quad \times \omega_0(W(F_{\mathbf{k}}^{(A)}\eta_{\mathbf{k}}^*(t)))\omega_0(W(F_{\mathbf{k}}^{(B)}\eta_{\mathbf{k}}^*(t))), \\
\rho_{18} &= e^{-2it(\Delta_A+\Delta_B+\Delta_C)} e^{-\Xi_{AB}} e^{-\Xi_{BC}} e^{-\Xi_{CA}} \\
&\quad \times \omega_0(W(F_{\mathbf{k}}^{(A)}\eta_{\mathbf{k}}^*(t)))\omega_0(W(F_{\mathbf{k}}^{(B)}\eta_{\mathbf{k}}^*(t))) \\
&\quad \times \omega_0(W(F_{\mathbf{k}}^{(C)}\eta_{\mathbf{k}}^*(t))) \\
\rho_{23} &= e^{-2it(\Delta_B-\Delta_C)} e^{i(\vartheta_{AB}-\vartheta_{CA})} e^{\Xi_{BC}} \\
&\quad \times \omega_0(W(F_{\mathbf{k}}^{(B)}\eta_{\mathbf{k}}^*(t)))\omega_0(W(F_{\mathbf{k}}^{(C)}\eta_{\mathbf{k}}^*(t))), \\
\rho_{24} &= e^{-2it(\Delta_A-\Delta_C)} e^{i(\vartheta_{AB}-\vartheta_{BC})} e^{\Xi_{CA}} \\
&\quad \times \omega_0(W(F_{\mathbf{k}}^{(C)}\eta_{\mathbf{k}}^*(t)))\omega_0(W(F_{\mathbf{k}}^{(A)}\eta_{\mathbf{k}}^*(t))), \\
\rho_{25} &= e^{-2it\Delta_B} e^{i(\vartheta_{AB}-\vartheta_{BC})} \omega_0(W(F_{\mathbf{k}}^{(B)}\eta_{\mathbf{k}}^*(t))), \\
\rho_{26} &= e^{-2it\Delta_A} e^{i(\vartheta_{AB}-\vartheta_{CA})} \omega_0(W(F_{\mathbf{k}}^{(A)}\eta_{\mathbf{k}}^*(t))), \\
\rho_{27} &= e^{-2it(\Delta_A+\Delta_B-\Delta_C)} e^{-\Xi_{AB}} e^{\Xi_{BC}} e^{\Xi_{CA}} \\
&\quad \times \omega_0(W(F_{\mathbf{k}}^{(A)}\eta_{\mathbf{k}}^*(t)))\omega_0(W(F_{\mathbf{k}}^{(B)}\eta_{\mathbf{k}}^*(t))) \\
&\quad \times \omega_0(W(F_{\mathbf{k}}^{(C)}\eta_{\mathbf{k}}^*(t))), \\
\rho_{28} &= e^{-2it(\Delta_A+\Delta_B)} e^{i(-\vartheta_{CA}-\vartheta_{BC})} e^{-\Xi_{AB}} \\
&\quad \times \omega_0(W(F_{\mathbf{k}}^{(A)}\eta_{\mathbf{k}}^*(t)))\omega_0(W(F_{\mathbf{k}}^{(B)}\eta_{\mathbf{k}}^*(t))), \\
\rho_{34} &= e^{-2it(\Delta_A-\Delta_B)} e^{i(\vartheta_{CA}-\vartheta_{BC})} e^{\Xi_{AB}}
\end{aligned}$$

$$\begin{aligned}
&\quad \times \omega_0(W(F_{\mathbf{k}}^{(A)}\eta_{\mathbf{k}}^*(t)))\omega_0(W(F_{\mathbf{k}}^{(B)}\eta_{\mathbf{k}}^*(t))), \\
\rho_{35} &= e^{-2it\Delta_C} e^{i(\vartheta_{CA}-\vartheta_{BC})} \omega_0(W(F_{\mathbf{k}}^{(C)}\eta_{\mathbf{k}}^*(t))), \\
\rho_{36} &= e^{-2it(\Delta_A-\Delta_B+\Delta_C)} e^{\Xi_{AB}} e^{\Xi_{BC}} e^{-\Xi_{CA}} \\
&\quad \times \omega_0(W(F_{\mathbf{k}}^{(A)}\eta_{\mathbf{k}}^*(t)))\omega_0(W(F_{\mathbf{k}}^{(B)}\eta_{\mathbf{k}}^*(t))) \\
&\quad \times \omega_0(W(F_{\mathbf{k}}^{(C)}\eta_{\mathbf{k}}^*(t))), \\
\rho_{37} &= e^{-2it\Delta_A} e^{i(-\vartheta_{AB}+\vartheta_{CA})} \omega_0(W(F_{\mathbf{k}}^{(A)}\eta_{\mathbf{k}}^*(t))), \\
\rho_{38} &= e^{-2it(\Delta_A+\Delta_C)} e^{i(-\vartheta_{AB}-\vartheta_{BC})} e^{-\Xi_{CA}} \\
&\quad \times \omega_0(W(F_{\mathbf{k}}^{(C)}\eta_{\mathbf{k}}^*(t)))\omega_0(W(F_{\mathbf{k}}^{(A)}\eta_{\mathbf{k}}^*(t))), \\
\rho_{45} &= e^{2it(\Delta_A-\Delta_B-\Delta_C)} e^{\Xi_{AB}} e^{-\Xi_{BC}} e^{\Xi_{CA}} \\
&\quad \times \omega_0(W(F_{\mathbf{k}}^{(A)}\eta_{\mathbf{k}}^*(t)))\omega_0(W(F_{\mathbf{k}}^{(B)}\eta_{\mathbf{k}}^*(t))) \\
&\quad \times \omega_0(W(F_{\mathbf{k}}^{(C)}\eta_{\mathbf{k}}^*(t))), \\
\rho_{46} &= e^{-2it\Delta_C} e^{i(-\vartheta_{CA}+\vartheta_{BC})} \omega_0(W(F_{\mathbf{k}}^{(C)}\eta_{\mathbf{k}}^*(t))), \\
\rho_{47} &= e^{-2it\Delta_B} e^{i(-\vartheta_{AB}+\vartheta_{BC})} \omega_0(W(F_{\mathbf{k}}^{(B)}\eta_{\mathbf{k}}^*(t))), \\
\rho_{48} &= e^{-2it(\Delta_B+\Delta_C)} e^{i(-\vartheta_{AB}-\vartheta_{CA})} e^{-\Xi_{BC}} \\
&\quad \times \omega_0(W(F_{\mathbf{k}}^{(B)}\eta_{\mathbf{k}}^*(t)))\omega_0(W(F_{\mathbf{k}}^{(C)}\eta_{\mathbf{k}}^*(t))), \\
\rho_{56} &= e^{-2it(\Delta_A-\Delta_B)} e^{i(-\vartheta_{CA}+\vartheta_{BC})} e^{\Xi_{AB}} \\
&\quad \times \omega_0(W(F_{\mathbf{k}}^{(A)}\eta_{\mathbf{k}}^*(t)))\omega_0(W(F_{\mathbf{k}}^{(B)}\eta_{\mathbf{k}}^*(t))), \\
\rho_{57} &= e^{-2it(\Delta_A-\Delta_C)} e^{i(-\vartheta_{AB}+\vartheta_{BC})} e^{\Xi_{CA}} \\
&\quad \times \omega_0(W(F_{\mathbf{k}}^{(C)}\eta_{\mathbf{k}}^*(t)))\omega_0(W(F_{\mathbf{k}}^{(A)}\eta_{\mathbf{k}}^*(t))), \\
\rho_{58} &= e^{-2it\Delta_A} e^{i(-\vartheta_{AB}-\vartheta_{CA})} \omega_0(W(F_{\mathbf{k}}^{(A)}\eta_{\mathbf{k}}^*(t))), \\
\rho_{67} &= e^{-2it(\Delta_B-\Delta_C)} e^{i(-\vartheta_{AB}+\vartheta_{CA})} e^{\Xi_{BC}} \\
&\quad \times \omega_0(W(F_{\mathbf{k}}^{(B)}\eta_{\mathbf{k}}^*(t)))\omega_0(W(F_{\mathbf{k}}^{(C)}\eta_{\mathbf{k}}^*(t))), \\
\rho_{68} &= e^{-2it\Delta_B} e^{i(-\vartheta_{AB}-\vartheta_{BC})} \omega_0(W(F_{\mathbf{k}}^{(B)}\eta_{\mathbf{k}}^*(t))), \\
\rho_{78} &= e^{-2it\Delta_C} e^{i(-\vartheta_{CA}-\vartheta_{BC})} \omega_0(W(F_{\mathbf{k}}^{(C)}\eta_{\mathbf{k}}^*(t))).
\end{aligned}$$

Here,  $\vartheta_{ij}, \omega_0(W(F_{\mathbf{k}}^{(j)}\eta_{\mathbf{k}}^*(t)))$ , and  $\Xi_{ij}$  are given in Eq. (B16), with appropriate coupling constants.

- 
- [1] W. G. Unruh, Notes on black-hole evaporation, Phys. Rev. D **14**, 870 (1976).
- [2] B. S. DeWitt, Quantum gravity: the new synthesis, in *General Relativity: An Einstein centenary survey*, edited by S. W. Hawking and W. Israel (Cambridge University Press, Cambridge, 1979) pp. 680–745.
- [3] S. W. Hawking, Particle creation by black holes, Comm. Math. Phys. **43**, 199 (1975).
- [4] R. Wald and J. Pfister, *Quantum Field Theory in Curved Spacetime and Black Hole Thermodynamics*, Chicago Lectures in Physics (University of Chicago Press, 1994).
- [5] L. C. B. Crispino, A. Higuchi, and G. E. A. Matsas, The Unruh effect and its applications, Rev. Mod. Phys. **80**, 787 (2008).
- [6] B. A. Juárez-Aubry and J. Louko, Onset and decay of the 1 + 1 Hawking-Unruh effect: what the derivative-coupling detector saw, Class. and Quantum Gravity **31**, 245007 (2014).
- [7] E. Tjoa and R. B. Mann, Unruh-DeWitt detector in dimensionally-reduced static spherically symmetric spacetimes, Journal of High Energy Physics **2022**, 1 (2022).
- [8] R. Lopp and E. Martín-Martínez, Quantum delocalization, gauge, and quantum optics: Light-matter interaction in relativistic quantum information, Phys. Rev. A **103**, 013703 (2021).
- [9] E. Martín-Martínez, T. R. Perche, and B. de S. L. Torres, General relativistic quantum optics: Finite-size particle detector models in curved spacetimes, Phys. Rev. D **101**, 045017 (2020).
- [10] T. R. Perche, Localized nonrelativistic quantum systems in curved spacetimes: A general characterization of particle detector models, Phys. Rev. D **106**, 025018 (2022).
- [11] N. Stritzelberger, L. J. Henderson, V. Baccetti, N. C.

- Menicucci, and A. Kempf, Entanglement harvesting with coherently delocalized matter, *Phys. Rev. D* **103**, 016007 (2021).
- [12] J. Doukas, S.-Y. Lin, B. Hu, and R. B. Mann, Unruh effect under non-equilibrium conditions: oscillatory motion of an Unruh-DeWitt detector, *Journal of High Energy Physics* **2013**, 1 (2013).
- [13] J.-T. Hsiang and B.-L. Hu, Quantum radiation and dissipation in relation to classical radiation and radiation reaction, *Phys. Rev. D* **106**, 045002 (2022).
- [14] M. Hotta, A. Kempf, E. Martín-Martínez, T. Tomitsuka, and K. Yamaguchi, Duality in the dynamics of Unruh-DeWitt detectors in conformally related spacetimes, *Phys. Rev. D* **101**, 085017 (2020).
- [15] T. R. Perche, J. Polo-Gómez, B. d. S. L. Torres, and E. Martín-Martínez, Particle detectors from localized quantum field theories, *Phys. Rev. D* **109**, 045013 (2024).
- [16] E. P. G. Gale and M. Zych, Relativistic Unruh-DeWitt detectors with quantized center of mass, *Phys. Rev. D* **107**, 056023 (2023).
- [17] C. Lima, E. Patterson, E. Tjoa, and R. B. Mann, Unruh phenomena and thermalization for qudit detectors, *Phys. Rev. D* **108**, 105020 (2023).
- [18] T. R. Perche, J. Polo-Gómez, B. d. S. L. Torres, and E. Martín-Martínez, Particle detectors from localized quantum field theories, *Phys. Rev. D* **109**, 045013 (2024).
- [19] E. Tjoa and K. Gallock-Yoshimura, Channel capacity of relativistic quantum communication with rapid interaction, *Phys. Rev. D* **105**, 085011 (2022).
- [20] A. G. S. Landulfo, Nonperturbative approach to relativistic quantum communication channels, *Phys. Rev. D* **93**, 104019 (2016).
- [21] P. Simidzija, A. Ahmadzadegan, A. Kempf, and E. Martín-Martínez, Transmission of quantum information through quantum fields, *Phys. Rev. D* **101**, 036014 (2020).
- [22] P. Simidzija, R. H. Jonsson, and E. Martín-Martínez, General no-go theorem for entanglement extraction, *Phys. Rev. D* **97**, 125002 (2018).
- [23] M. Kasprzak and E. Tjoa, Transmission of quantum information through quantum fields in curved spacetimes, *Journal of Physics A: Mathematical and Theoretical* **58**, 095301 (2025).
- [24] J. Polo-Gómez and E. Martín-Martínez, Nonperturbative method for particle detectors with continuous interactions, *Phys. Rev. D* **109**, 045014 (2024).
- [25] K. Gallock-Yoshimura, Y. Osawa, and Y. Nambu, Acceleration-induced radiation from a qudit particle detector model, *Phys. Rev. D* **111**, 105012 (2025).
- [26] I. B. Barcellos and A. G. S. Landulfo, Relativistic quantum broadcast channel, *Phys. Rev. D* **109**, 065020 (2024).
- [27] E. Tjoa, Nonperturbative simple-generated interactions with a quantum field for arbitrary Gaussian states, *Phys. Rev. D* **108**, 045003 (2023).
- [28] D. M. Avalos, K. Gallock-Yoshimura, L. J. Henderson, and R. B. Mann, Instant extraction of nonperturbative tripartite entanglement, *Phys. Rev. Res.* **5**, L042039 (2023).
- [29] E. Tjoa and F. Gray, The Unruh-DeWitt model and its joint interacting Hilbert space, *Journal of Physics A: Mathematical and Theoretical* **57**, 325301 (2024).
- [30] A. Amann, Ground states of a spin-boson model, *Annals of Physics* **208**, 414 (1991).
- [31] H. Spohn, Ground state(s) of the spin-boson Hamiltonian, *Communications in Mathematical Physics* **123**, 277 (1989).
- [32] M. Fannes, B. Nachtergaele, and A. Verbeure, The equilibrium states of the spin-boson model, *Communications in mathematical physics* **114**, 537 (1988).
- [33] S. Takagi, Vacuum Noise and Stress Induced by Uniform Acceleration, Hawking-Unruh Effect in Rindler Manifold of Arbitrary Dimension, *Progress of Theoretical Physics Supplement* **88**, 1 (1986).
- [34] N. Birrell and P. Davies, *Quantum Fields in Curved Space*, Cambridge Monographs on Mathematical Physics (Cambridge University Press, 1984).
- [35] W. G. Unruh and R. M. Wald, What happens when an accelerating observer detects a rindler particle, *Phys. Rev. D* **29**, 1047 (1984).
- [36] P. Simidzija and E. Martín-Martínez, All coherent field states entangle equally, *Phys. Rev. D* **96**, 025020 (2017).
- [37] T. R. Perche, Closed-form expressions for smeared bidistributions of a massless scalar field: Nonperturbative and asymptotic results in relativistic quantum information, *Phys. Rev. D* **110**, 025013 (2024).
- [38] R. G. McLenaghan, On the validity of Huygens' principle for second order partial differential equations with four independent variables. Part I : derivation of necessary conditions, *Annales de l'I.H.P. Physique théorique* **20**, 153 (1974).
- [39] S. Sonego and V. Faraoni, Huygens' principle and characteristic propagation property for waves in curved spacetimes, *Journal of Mathematical Physics* **33**, 625 (1992).
- [40] V. Faraoni, Massive spin zero fields in cosmology and the tail-free property, *Symmetry* **11**, 10.3390/sym11010036 (2019).
- [41] E. Tjoa and E. Martín-Martínez, When entanglement harvesting is not really harvesting, *Phys. Rev. D* **104**, 125005 (2021).
- [42] D. Mendez-Avalos, L. J. Henderson, K. Gallock-Yoshimura, and R. B. Mann, Entanglement harvesting of three Unruh-DeWitt detectors, *General Relativity and Gravitation* **54**, 87 (2022).
- [43] I. J. Membrere, K. Gallock-Yoshimura, L. J. Henderson, and R. B. Mann, Tripartite Entanglement Extraction from the Black Hole Vacuum, *Advanced Quantum Technologies* **6**, 2300125 (2023).
- [44] T.-P. Hack, *Cosmological applications of algebraic quantum field theory in curved spacetimes*, Vol. 6 (Springer, 2015).
- [45] C. J. Fewster and K. Rejzner, Algebraic quantum field theory – an introduction (2019), arXiv:1904.04051 [hep-th].
- [46] B. S. Kay and R. M. Wald, Theorems on the uniqueness and thermal properties of stationary, nonsingular, quasifree states on spacetimes with a bifurcate killing horizon, *Physics Reports* **207**, 49 (1991).
- [47] I. Khavkine and V. Moretti, Algebraic QFT in curved spacetime and quasifree Hadamard states: An introduction, *Mathematical Physics Studies*, 191–251 (2015).
- [48] O. Bratteli and D. Robinson, *Operator Algebras and Quantum Statistical Mechanics: Vol. 2: Models in quantum statistical mechanics.*, 2nd ed., Texts and Monographs in Physics, Vol. 2 (Springer, 2002).
- [49] D. Hasler and I. Herbst, Ground states in the spin boson model, in *Annales Henri Poincaré*, Vol. 12 (Springer, 2011) pp. 621–677.
- [50] D. Hasler, B. Hinrichs, and O. Siebert, On existence of

- ground states in the spin boson model, *Communications in Mathematical Physics* **388**, 419 (2021).
- [51] M. J. Radzikowski, Micro-local approach to the Hadamard condition in quantum field theory on curved space-time, *Communications in Mathematical Physics* **179**, 529 (1996).
- [52] C. J. Fewster and R. Verch, The necessity of the hadamard condition, *Classical and Quantum Gravity* **30**, 235027 (2013).
- [53] C. J. Fewster, Hadamard states for decomposable green-hyperbolic operators, arXiv:2503.12537 (2025).
- [54] E. Witten, Why does quantum field theory in curved spacetime make sense? And what happens to the algebra of observables in the thermodynamic limit?, in *Dialogues Between Physics and Mathematics: CN Yang at 100* (Springer, 2022) pp. 241–284.
- [55] M. H. Rued, Weakly coupled local particle detectors cannot harvest entanglement, *Classical and Quantum Gravity* **38**, 195029 (2021).
- [56] E. Poisson, A. Pound, and I. Vega, The motion of point particles in curved spacetime, *Living Reviews in Relativity* **14**, 1 (2011).
- [57] S. De Bievre and M. Merkli, The Unruh effect revisited, *Classical and Quantum Gravity* **23**, 6525 (2006).
- [58] E. Martín-Martínez, Causality issues of particle detector models in QFT and quantum optics, *Phys. Rev. D* **92**, 104019 (2015).
- [59] E. Martín-Martínez, T. R. Perche, and B. d. S. L. Torres, Broken covariance of particle detector models in relativistic quantum information, *Phys. Rev. D* **103**, 025007 (2021).
- [60] J. de Ramón, M. Papageorgiou, and E. Martín-Martínez, Relativistic causality in particle detector models: Faster-than-light signaling and impossible measurements, *Phys. Rev. D* **103**, 085002 (2021).
- [61] J. de Ramón, M. Papageorgiou, and E. Martín-Martínez, Causality and signalling in noncompact detector-field interactions, *Phys. Rev. D* **108**, 045015 (2023).
- [62] A. G. Passegger and R. Verch, Disjointness of inertial KMS states and the role of Lorentz symmetry in thermalization, *Reviews in Mathematical Physics* **37**, 2430009 (2025).
- [63] C. J. Fewster, B. A. Juárez-Aubry, and J. Louko, Waiting for Unruh, *Classical and Quantum Gravity* **33**, 165003 (2016).
- [64] R. H. Jonsson, D. Q. Aruquipa, M. Casals, A. Kempf, and E. Martín-Martínez, Communication through quantum fields near a black hole, *Phys. Rev. D* **101**, 125005 (2020).
- [65] H. Maeso-García, J. Polo-Gómez, and E. Martín-Martínez, Entanglement harvesting: State dependence and covariance, *Phys. Rev. D* **106**, 105001 (2022).
- [66] A. Blasco, L. J. Garay, M. Martín-Benito, and E. Martín-Martínez, Violation of the Strong Huygen’s Principle and Timelike Signals from the Early Universe, *Phys. Rev. Lett.* **114**, 141103 (2015).
- [67] A. Blasco, L. J. Garay, M. Martín-Benito, and E. Martín-Martínez, Timelike information broadcasting in cosmology, *Phys. Rev. D* **93**, 024055 (2016).
- [68] E. Tjoa and E. Martín-Martínez, Zero mode suppression of superluminal signals in light-matter interactions, *Phys. Rev. D* **99**, 065005 (2019).
- [69] E. Martín-Martínez and J. Louko, Particle detectors and the zero mode of a quantum field, *Phys. Rev. D* **90**, 024015 (2014).
- [70] B. Allen and A. Folacci, Massless minimally coupled scalar field in de Sitter space, *Phys. Rev. D* **35**, 3771 (1987).
- [71] H. Araki and E. Woods, Representations of the canonical commutation relations describing a nonrelativistic infinite free Bose gas, *Journal of Mathematical Physics* **4**, 637 (1963).
- [72] E. Morfa-Morales, Deformations of quantum field theories on curved spacetimes, arXiv:1202.3278 (2012).
- [73] A. Pozas-Kerstjens and E. Martín-Martínez, Harvesting correlations from the quantum vacuum, *Phys. Rev. D* **92**, 064042 (2015).
- [74] A. Pozas-Kerstjens and E. Martín-Martínez, Entanglement harvesting from the electromagnetic vacuum with hydrogenlike atoms, *Phys. Rev. D* **94**, 064074 (2016).
- [75] B. Reznik, Entanglement from the vacuum, *Found. Phys.* **33**, 167 (2003).
- [76] B. Reznik, A. Retzker, and J. Silman, Violating Bell’s inequalities in vacuum, *Phys. Rev. A* **71**, 042104 (2005).
- [77] A. Valentini, Non-local correlations in quantum electrodynamics, *Phys. Lett. A* **153**, 321 (1991).
- [78] J. G. A. Caribé, R. H. Jonsson, M. Casals, A. Kempf, and E. Martín-Martínez, Lensing of vacuum entanglement near Schwarzschild black holes, *Phys. Rev. D* **108**, 025016 (2023).
- [79] A. Pozas-Kerstjens, J. Louko, and E. Martín-Martínez, Degenerate detectors are unable to harvest spacelike entanglement, *Phys. Rev. D* **95**, 105009 (2017).
- [80] M. Scully and M. Zubairy, *Quantum Optics*, Quantum Optics (Cambridge University Press, 1997).
- [81] V. Vedral, *Modern foundations of quantum optics* (Imperial College Press, 2005).
- [82] E. Martín-Martínez and T. R. Perche, What gravity mediated entanglement can really tell us about quantum gravity, *Phys. Rev. D* **108**, L101702 (2023).
- [83] A. Retzker, J. I. Cirac, and B. Reznik, Detecting vacuum entanglement in a linear ion trap, *Phys. Rev. Lett.* **94**, 050504 (2005).
- [84] A. Teixidó-Bonfill, X. Dai, A. Lupascu, and E. Martín-Martínez, Towards an experimental implementation of entanglement harvesting in superconducting circuits: effect of detector gap variation on entanglement harvesting, arXiv:2505.01516 (2025).
- [85] F. Lindel, A. Herter, V. Gebhart, J. Faist, and S. Y. Buhmann, Entanglement harvesting from electromagnetic quantum fields, *Phys. Rev. A* **110**, 022414 (2024).
- [86] Y.-C. Ou and H. Fan, Monogamy inequality in terms of negativity for three-qubit states, *Phys. Rev. A* **75**, 062308 (2007).
- [87] J. Silman and B. Reznik, Many-region vacuum entanglement: Distilling a  $W$  state, *Phys. Rev. A* **71**, 054301 (2005).
- [88] A. Acín, A. Andrianov, L. Costa, E. Jané, J. I. Latorre, and R. Tarrach, Generalized Schmidt Decomposition and Classification of Three-Quantum-Bit States, *Phys. Rev. Lett.* **85**, 1560 (2000).
- [89] S. Xie and J. H. Eberly, Triangle measure of tripartite entanglement, *Phys. Rev. Lett.* **127**, 040403 (2021).
- [90] V. Coffman, J. Kundu, and W. K. Wootters, Distributed entanglement, *Phys. Rev. A* **61**, 052306 (2000).
- [91] A. Acín, D. Bruß, M. Lewenstein, and A. Sanpera, Classification of mixed three-qubit states, *Phys. Rev. Lett.* **87**, 040401 (2001).
- [92] L. van Luijk, A. Stottmeister, and H. Wilming, Multi-

- partite embezzlement of entanglement, arXiv:2409.07646 (2024).
- [93] Y. Uenaga, K. Gallock-Yoshimura, and T. Taira, Exact treatment of the quantum Langevin equation under time-dependent system-bath coupling via a train of delta distributions, arXiv:2505.00386 (2025).
- [94] R. Gilmore, *Lie Groups, Physics, and Geometry: An Introduction for Physicists, Engineers and Chemists* (Cambridge University Press, 2008).
- [95] DLMF, *NIST Digital Library of Mathematical Functions*, <http://dlmf.nist.gov/>, Release 1.0.27 of 2020-06-15, f. W. J. Olver, A. B. Olde Daalhuis, D. W. Lozier, B. I. Schneider, R. F. Boisvert, C. W. Clark, B. R. Miller, B. V. Saunders, H. S. Cohl, and M. A. McClain, eds.
- [96] M. Abramowitz and I. Stegun, *Handbook of Mathematical Functions: With Formulas, Graphs, and Mathematical Tables*, Applied mathematics series (Dover Publications, 1965).